The Kuramoto model with inertia: from fireflies to power grids

Simona Olmi

Istituto dei Sistemi Complessi - CNR - Firenze, Italy

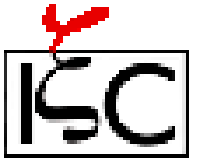

Pteroptix Malaccae

- A phase model with inertia has been introduced to mimic the synchronization mechanisms observed among the Malaysian fireflies Pteroptix Malaccae. These fireflies synchronize their flashing activity by entraining to the forcing frequency with almost zero phase lag. Usually, entrainment results in a constant phase angle equal to the difference between pacing frequency and free-running period as it does in P. cribellata.
  (B. Ermentrout (1991), Experiments by Hanson, (1987))

Why introducing “inertia”?

- First-order Kuramoto model
  - It approaches too fast the partial synchronized state
  - Infinite coupling strength is required to achive full synchronization

- Second-order Kuramoto model
  - Synchronization is slowed down by inertia (frequency adaptation)
  - Firstly proposed in biological context (Ermentrout, (1991))
  - Used to study synchronization in disordered arrays of Josephson junctions (Strogatz (1994), Trees et al. (2005))
  - Derived from the classical swing equation to study synchronization in power grids (Filatrella et al. (2008))

The Model

Kuramoto model with inertia

$$m\ddot{\theta}_i + \dot{\theta}_i = \Omega_i + \frac{K}{N}\sum_j \sin(\theta_j - \theta_i)$$

- θ_i is the instantaneous phase
- Ω_i is the natural frequency of the $i-$th oscillator with Gaussian distribution
- K is the coupling constant
- N is the number of oscillators

By introducing the complex order parameter $r(t)e^{i\phi(t)} = \frac{1}{N}\sum_j e^{i\theta_j}$

$$m\ddot{\theta}_i + \dot{\theta}_i = \Omega_i - Kr\sin(\theta_i - \phi)$$

$r = 0$ asynchronous state, $r = 1$ synchronized state

Damped Driven Pendulum

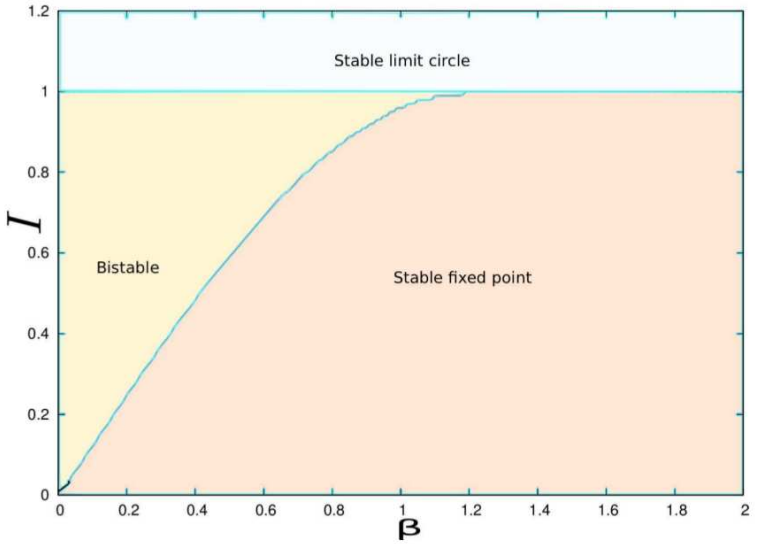

$$m\ddot{\theta}_i + \dot{\theta}_i = \Omega_i - Kr\sin(\theta_i)$$

$$I = \frac{\Omega_i}{Kr}$$
$$\beta = \frac{1}{\sqrt{mKr}}$$

$$\ddot{\phi} + \beta\dot{\phi} = I - \sin(\phi)$$

- One node connected to the grid (the grid is considered to be infinite)
- Single damped driven pendulum
- Josephson junctions
- One-machine infinite bus system of a generator in a power-grid (Chiang, (2011))

Damped Driven Pendulum

$$\ddot{\phi} + \beta\dot{\phi} = I - \sin(\phi)$$

For sufficiently large m (small β)

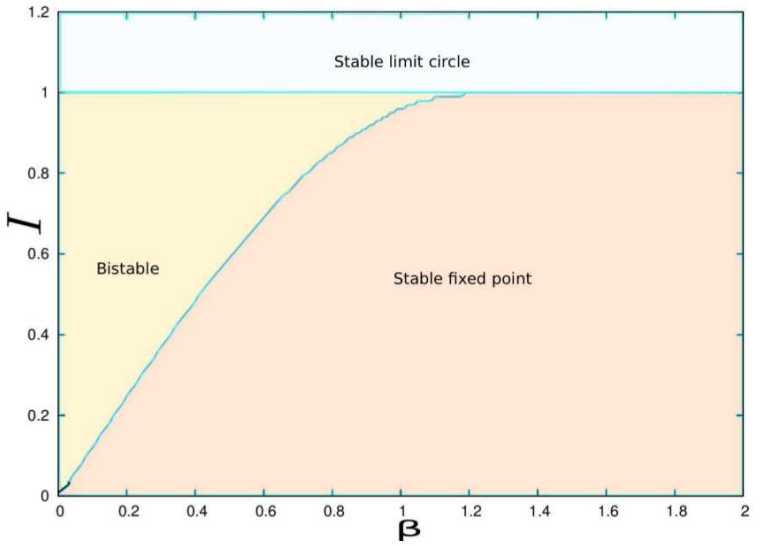

- For small Ω_i two fixed points are present: a stable node and a saddle. The linear stability is given by

$$J = \begin{pmatrix} 0 & 1 \\ -\cos\phi^* & -\beta \end{pmatrix}$$

$$\sigma_{1,2} = \frac{-\beta \pm \sqrt{\beta^2 - 4\cos\phi^*}}{2}$$

- At large frequencies $\Omega_i > \Omega_P = \frac{4}{\pi}\sqrt{\frac{Kr}{m}}$ (i.e. $I > \frac{4\beta}{\pi}$) a limit cycle emerges from the saddle via a homoclinic bifurcation

- Limit cycle and fixed point coexists until $\Omega_i \equiv \Omega_D = Kr$ (i.e. $I = 1$), where a saddle node bifurcation leads to the disappearence of the two fixed points
- For $\Omega_i > \Omega_D$ (i.e. $I > 1$) only the oscillating solution is present

For small mass (large β), there is no more coexistence.
(Levi et al. 1978)

Simulation Protocols

Dynamics of N oscillators (first order transition and hysteresis)

- Ω_M maximal natural frequency of the locked oscillators
- $\Omega_P^{(I)} = \frac{4}{\pi}\sqrt{\frac{Kr}{m}}$
- $\Omega_D^{(II)} = Kr$

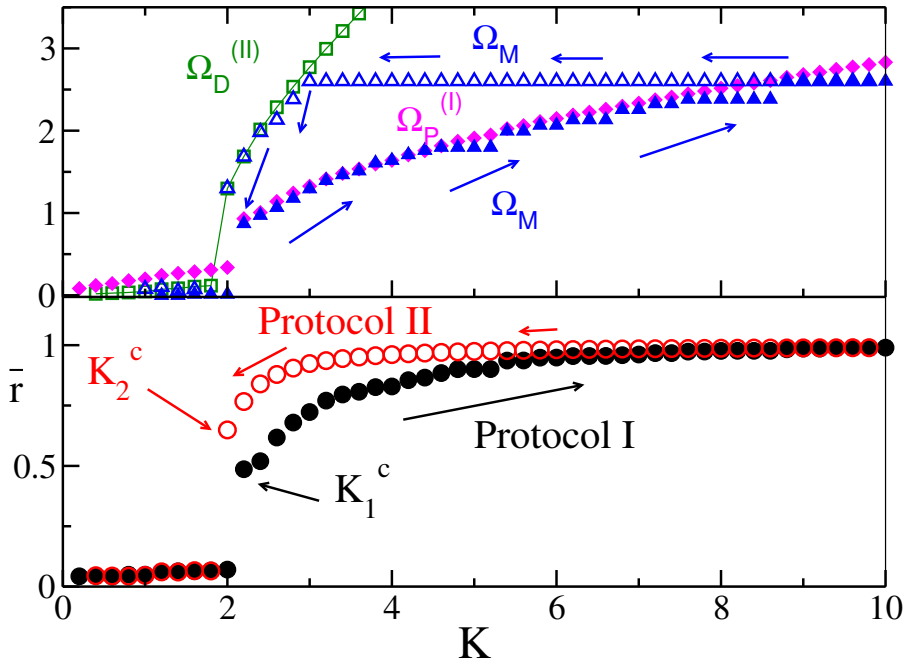

$m = 2$

Protocol I: Increasing K

The system remains desynchronized until $K = K_c^1$ (filled black circles). Ω_M increases with K following Ω_P^I. Ω_i are grouped in small clusters (plateaus).

Protocol II: Decreasing K

The system remains synchronized until $K = K_c^2$ (empty black circles). Ω_M remains stucked to the same value for a large K interval than it rapidly decreases to 0 following Ω_D^{II}.

Mean Field Theory (Tanaka et al. (1997))

$$m\ddot{\theta}_i + \dot{\theta}_i = \Omega_i - Kr\sin(\theta_i - \phi)$$

- by following Protocol I and II there is a group of drifting oscillators and one of locked oscillators which act separately
  - locked oscillators are characterized by $< \dot{\theta} >= 0$ and are locked to the mean phase
  - drifting oscillators (with $< \dot{\theta} >\neq 0$) are whirling over the locked subgroup (or below depending on the sign of Ω_i)
- Drifting and locked oscillators are separated by a certain frequency:
  - Following Protocol I the oscillators with $\Omega_i < \Omega_P$ are locked
  - Following Protocol II the oscillators with $\Omega_i < \Omega_D$ are locked
- These two groups contribute differently to the total level of synchronization in the system

$$r = r_L + r_D$$

Mean Field Theory (Tanaka et al. (1997))

Protocol I: $\Omega_P^{(I)} = \frac{4}{\pi}\sqrt{\frac{Kr}{m}}$

- All oscillators initially drift around its own natural frequency Ω_i
- Increasing K, oscillators with $\Omega_i < \Omega_P$ are attracted by the locked group
- Increasing K also Ω_P increases $\Rightarrow$ oscillators with bigger Ω_i become synchronized
- The phase coherence r^I increases and Ω_i exhibits plateaus
- ! Depending on m the transition to synchronization may increase in complexity

Protocol II: $\Omega_D^{(II)} = Kr$

- Oscillators are initially locked to the mean phase and $r^{II} \approx 1$
- Decreasing K, locked oscillators are desynchronized and start whirling when $\Omega_i > \Omega_D$ and a saddle node bifurcation occurs

Ω_P, Ω_D are the synchronization boundaries

Mean Field Theory (Tanaka et al. (1997))

Total level of synchronization in the system: $r = r_L + r_D$

For the locked population the self-consistent equation is

$$r_L^{I,II} = Kr \int_{-\theta_{P,D}}^{\theta_{P,D}} \cos^2\theta \; g(Kr\sin\theta)d\theta$$

where $\theta_P = \sin^{-1}(\frac{\Omega_P}{Kr})$, $\theta_D = \sin^{-1}(\frac{\Omega_D}{Kr}) = \pi/2$, $g(\Omega)$ frequency distribution.

The drifting population contributes to the total order parameter with a negative contribution

$$r_D^{I,II} \simeq -mKr \int_{-\Omega_{P,D}}^{\infty} \frac{1}{(m\Omega)^3} g(\Omega)d\Omega$$

The former equation are correct in the limit of sufficiently large masses

Hysteretic Behavior

Numerical Results for Fully Coupled Networks ($N = 500$, $m = 6$)

- The data obtained by following protocol II are quite well reproduced by the mean field approximation r^{II}
- The mean field extimation r^{I} does not reproduce the stepwise structure numerically obtained in protocol I

- Clusters of N_L locked oscillators of any size remain stable between r^{I} and r^{II}
- The level of synchronization of these clusters can be theoretically obtained by generalizing the theory of Tanaka et al. (1997) to protocols where Ω_M remains constant

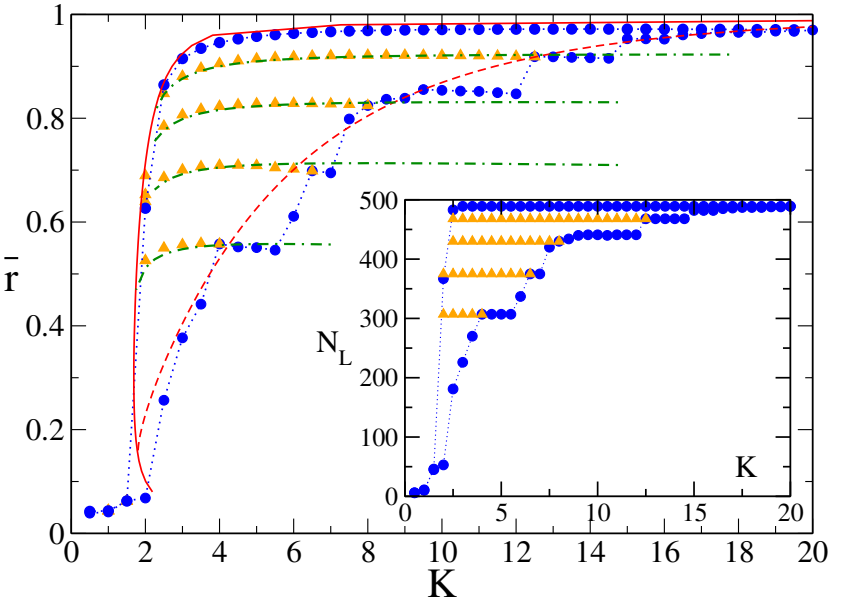

(Olmi et al. (2014))

Finite Size Effects

- K_1^c is the transition value from asynchronous to synchronous state (following Protocol I)
- K_2^c is the transition value from synchronous to asynchronous state (following Protocol II)

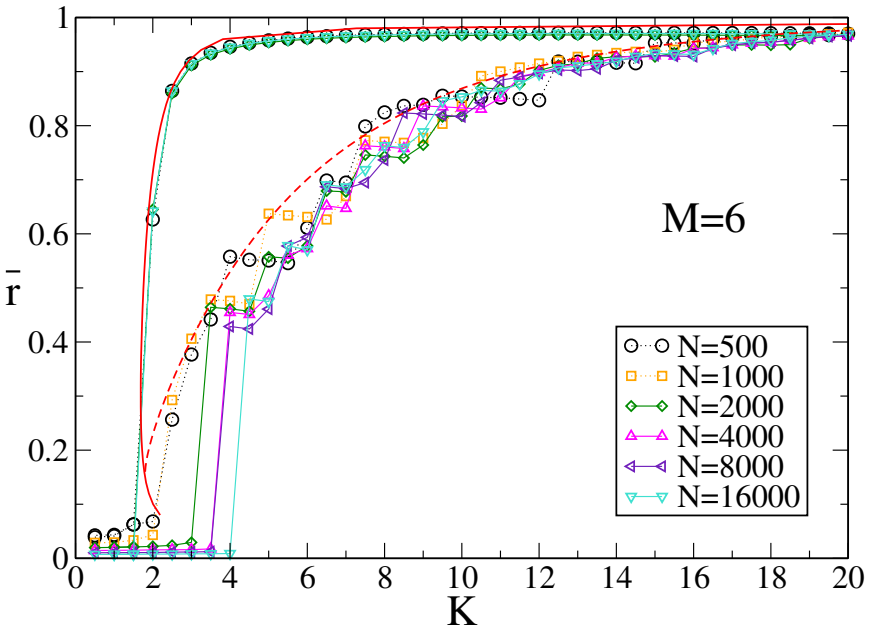

Finite Size Effects (Olmi et al. (2014))

- a) $m = 0.8$, (b) $m = 1$, (c) $m = 2$ and (d) $m = 6$
- K_1^c (upper points) is strongly influenced by the size of the system
- K_2^c (lower points) does not depend heavily on N
- Good agreement between Mean Field and simulations is achieved for small m
- For large m the emergence of the secondary synchronization of drifting oscillators (i.e. clusters of whirling oscillators) is determinant

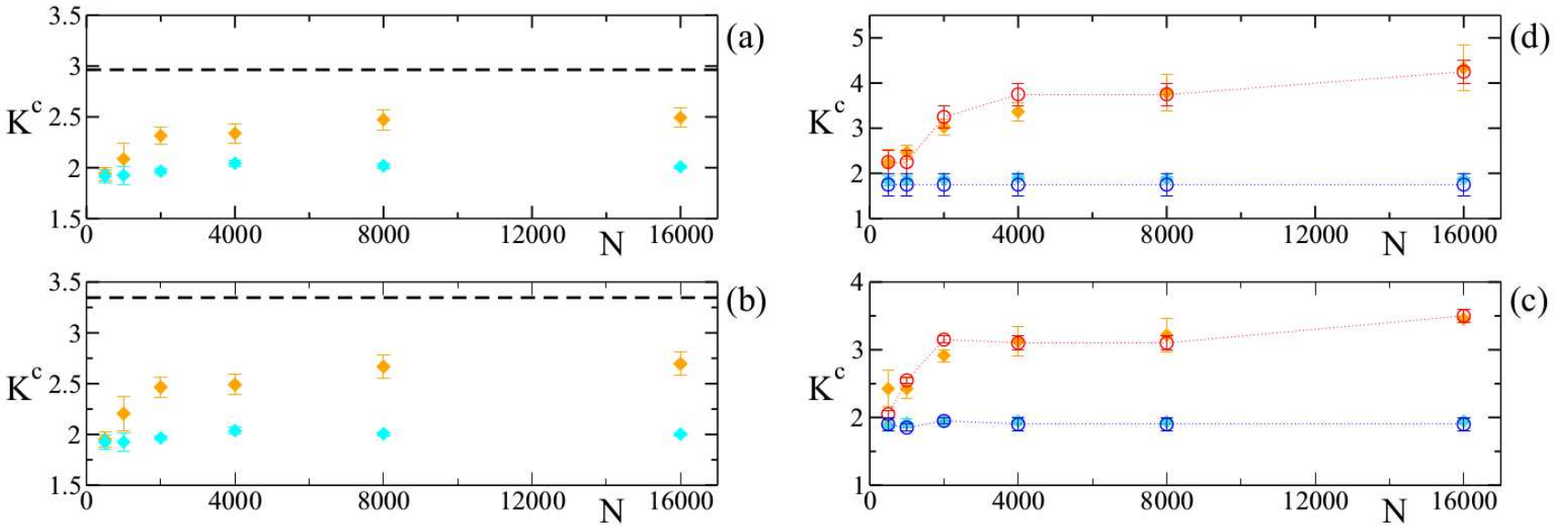

Dashed line $\rightarrow K_1^{MF}$ mean field value by Gupta et al (PRE 2014)

Drifting Clusters

For larger masses (m=6), the synchronization transition becomes more complex, it occurs via the emergence of clusters of drifting oscillators.

The partially synchronized state is characterized by the coexistence of

- a cluster of locked oscillators with $< \dot{\theta} > \simeq 0$
- clusters composed by drifting oscillators with finite average velocities

Extra clusters induce (periodic or quasi-periodic) oscillations in the temporal evolution of $r(t)$.

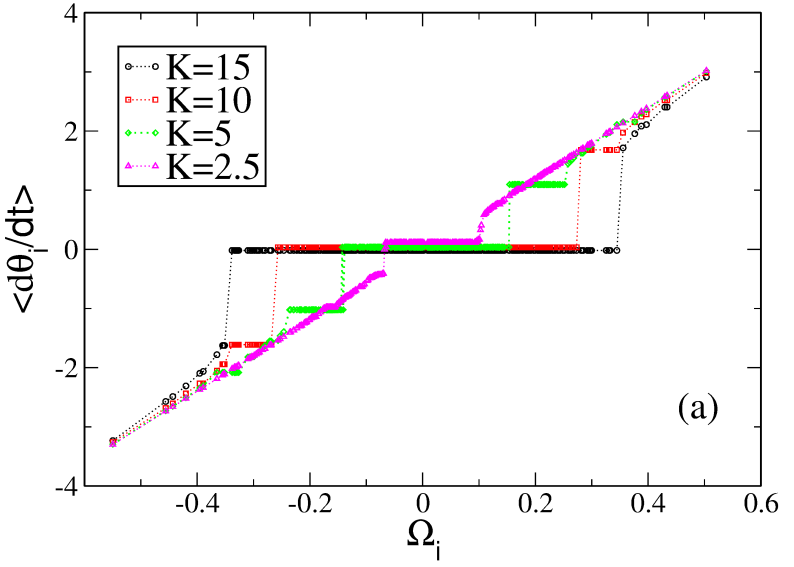

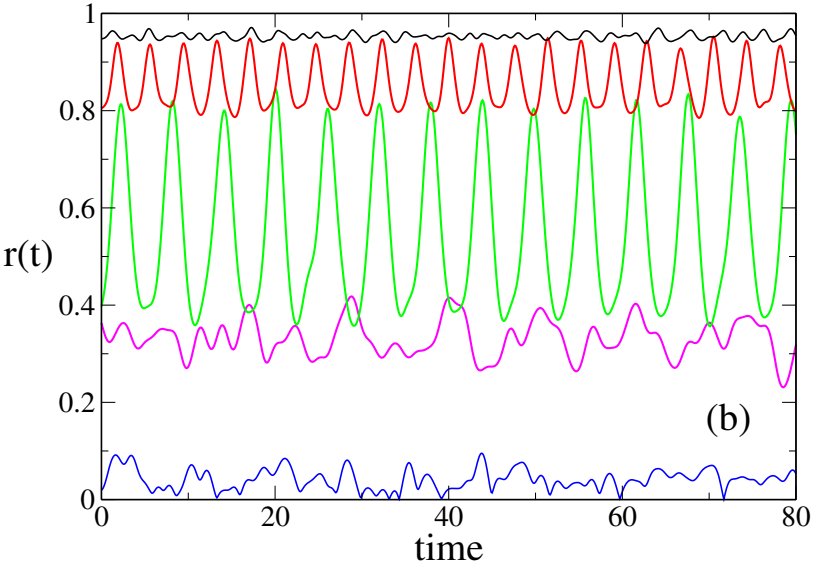

(Olmi et al. (2014))

Drifting Clusters

If we compare the evolution of the instantaneous velocities $\dot{\theta}_i$ for 3 oscillators and $r(t)$ we observe that

- the phase velocities of O_2 and O_3 display synchronized motion
- the phase velocity of O_1 oscillates irregularly around zero
- the oscillations of $r(t)$ are driven by the periodic oscillations of O_2 and O_3

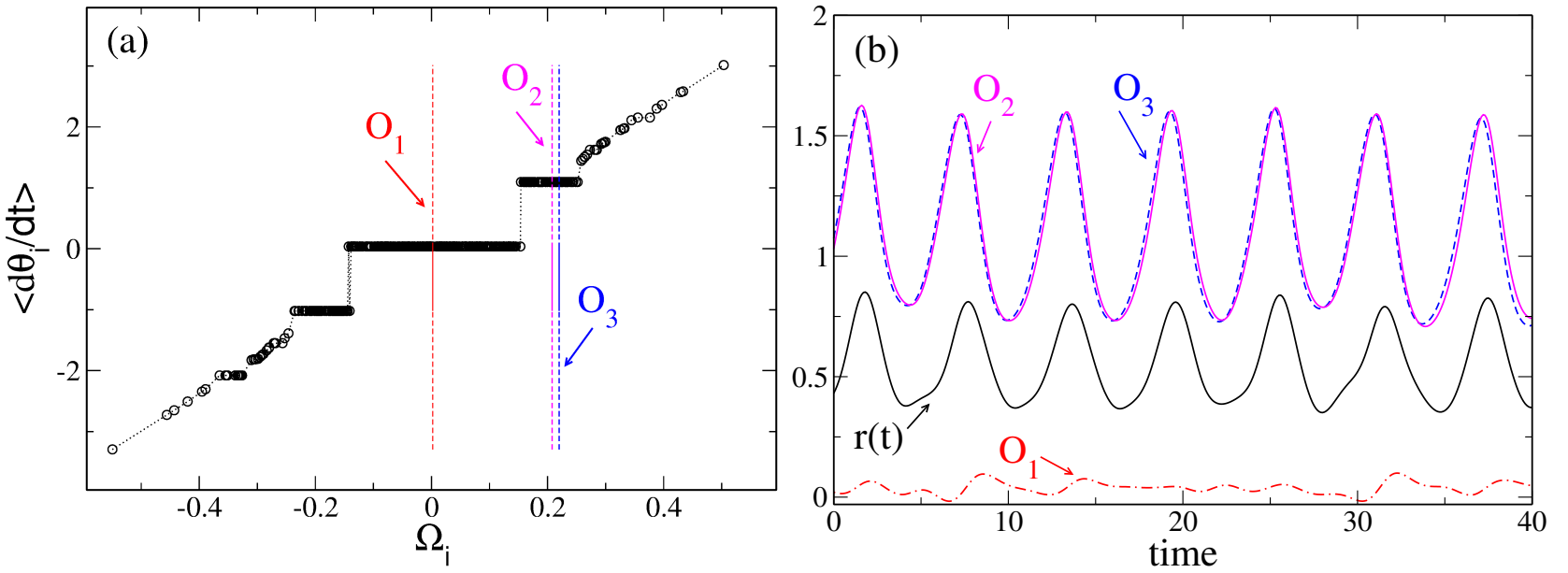

(Olmi et al. (2014))

Power Grids

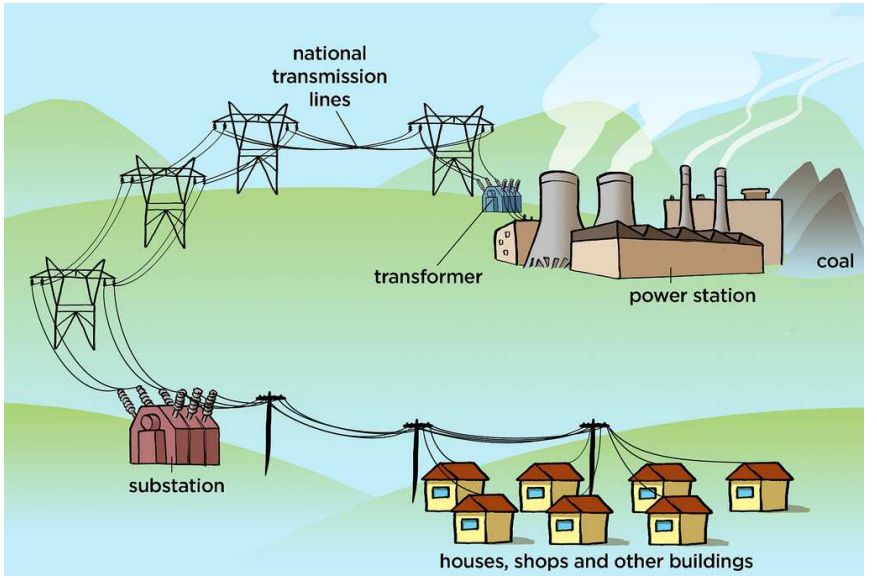

- Power Plants
- Swing Equation

- Decentralization
- Turbulent Character of Renewable Sources
- Control

Power Plants

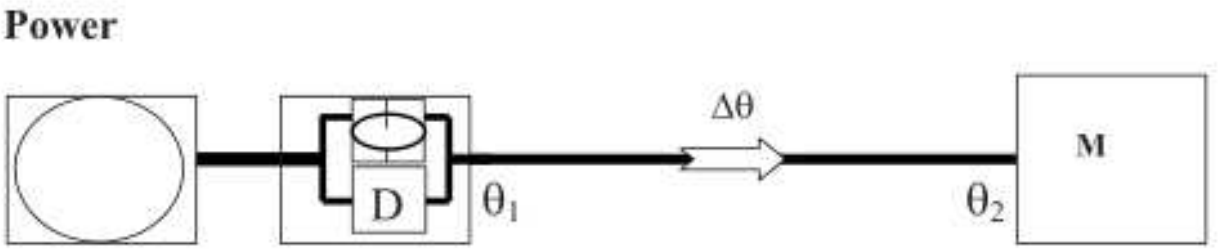

Fig. 1. Equivalent diagram of generator and machine connected by a transmission line. The turbine consists of a flywheel and dissipation D.

- A power plant consist of a boiler producing a constant power, as well as a turbine (generator) with high inertia and some damping.
- Transmitted power through a line: $P_{12}^{max} sin(\theta_2 - \theta_1)$.
- Power plant + transmission line =power source that feeds energy into the system. This energy can be accumulated as rotational energy or dissipated due to friction.
- The remaining part is available for a user (the machine M), provided that there exists a phase angle difference $\Delta\theta = \theta_2 - \theta_1$ between the two mechanical rotators (phase shift is necessary for ac power transmission)

Power grids: swing equation

Power flow analysis can be described in terms of the phase angles $\theta's$ that characterize both the rotor dynamics (and hence the energy stored or dissipated) and the power flow between any two rotors connected by an ac line.

$$\theta_i(t) = \Omega t + \phi_i(t), \qquad \Omega = 2\pi \times 50Hz$$

$$P_i^{source} = P_i^{diss} + P_i^{acc} + P_i^{transmitted}$$

$$P_i^{diss} = k_i^D \dot{\theta_i}^2, \qquad P_i^{acc} = \frac{1}{2} I_i \frac{d^2\theta_i}{dt^2}, \qquad P_i^{transmitted} = P_{ij}^{max} \sin(\theta_j - \theta_i)$$

Assuming only slow phase changes compared to the frequency ($|\dot{\theta_i}| \ll \Omega$)

$$I_i \Omega \ddot{\phi}_i = P_i^{source} - k_i^D \Omega^2 - 2k_i \Omega \dot{\phi} + \sum_j P_{ij}^{max} \sin(\theta_j - \theta_i)$$

only the phase difference between the elements of the grid matters!

(Filatrella et al. (2008))

Power grids: parameters

Every element i is described by the same rescaled equation of motion with a parameter P_i giving the generated $(P_i > 0)$ or consumed $(P_i < 0)$ power

$$\frac{d^2\phi_i}{dt^2} = P_i - \alpha_i \frac{d\phi}{dt} + \sum_j K_{ij} \sin(\theta_j - \theta_i)$$

where $K_{ij} = \frac{P_{ij}^{max}}{I_i \Omega}$, $P_i = \frac{P_i^{source} - k_i^D \Omega^2}{I_i \Omega}$, $\alpha_i = \frac{2k_i}{I_i}$, $\sum_j P_j = 0$.

- Large centralized power plants generating $P_i^{source} = 100Mw$ each
- Each synchronous generator has a moment of inertia of $I_i = 10^4 kgm^2$
- The mechanically dissipated power $k_i^D \Omega^2$ usually is a small fraction of P^{source}
- Additional sources of dissipation are not taken into account
- A transmission capacity for major overhead power line is up to $P_{ij}^{max} = 700MW$
- The transmission capacity for a line connecting a small city is $K_{ij} \leq 10^2 s^{-2}$
- $\alpha_i = 0.1s^{-1}$, $P_i = 10s^{-2}$ for large power plants, $P_i = -1s^{-2}$ for a small city

Decentralization: Real Grid (Rohden et al. (2012))

- Larger networks of complex topologies equally exhibit coexistence with power outage and self-organized synchrony
- Average frequency $\omega = \sum_j |d\phi_j/dt|/N$
- Order parameter $r(t) = \sum_j e^{i\phi_j}(t)/N$
- Topology of the British power grid: 120 nodes and 165 transmission lines; 10 power plants (randomly chosen) and 110 consumers
- Power plants are connected to their neighbors with a higher capacity cK

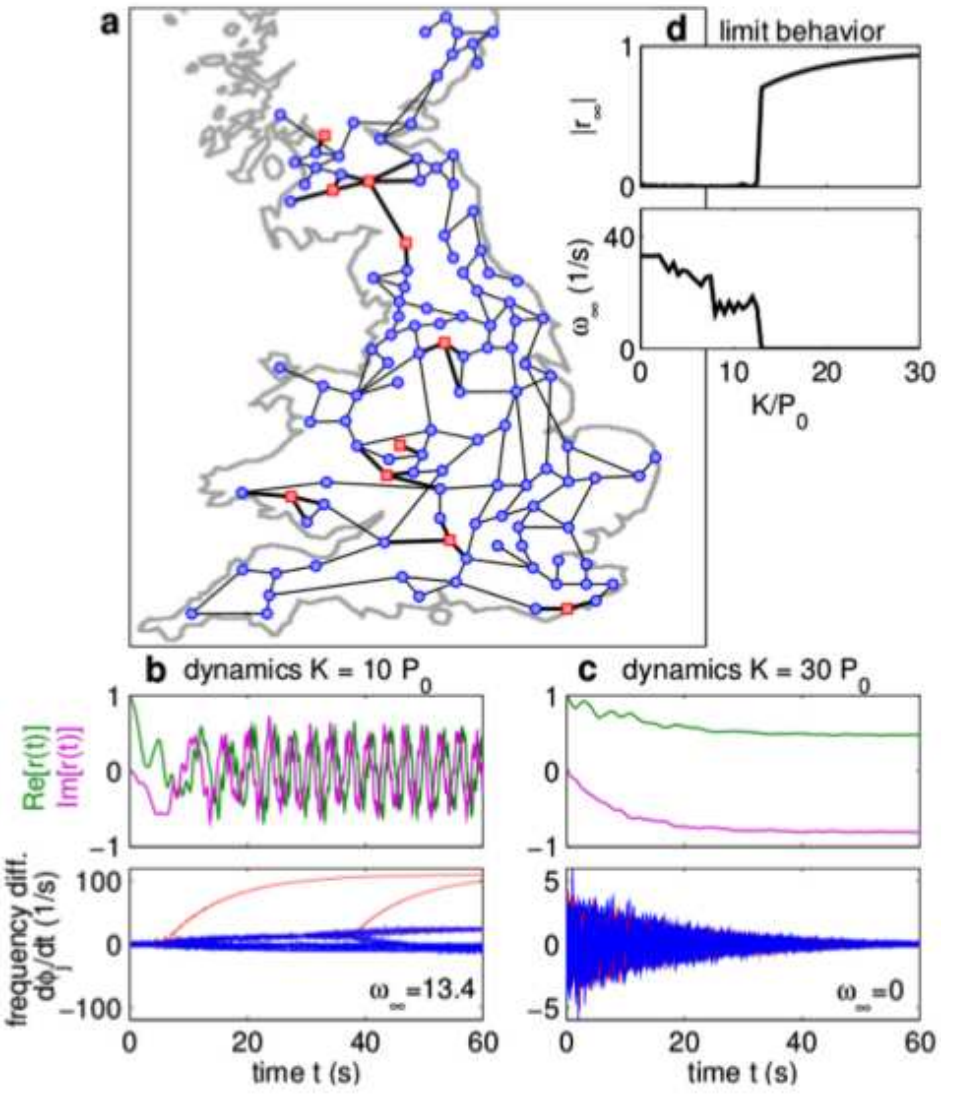

Decentralization: Stability (Rohden et al. (2012))

How does decentralization impact the system's stability to dynamic perturbations?

- Replace large power plants ($P_j = 11P_0$) by smaller ones ($P_j = 1.1P_0$).
- Test the stability against fluctuations by transiently increasing the power demand of each consumer during a short time interval (the condition $\sum_j P_j = 0$ is violated)
- After the perturbation is switched off, the system either relaxes back to a steady state or does not, depending on the strength of the perturbation
- The maximally allowed perturbation strength shrinks with decentralization, but still all grids are stable up to strengths a few times larger than the unperturbed load

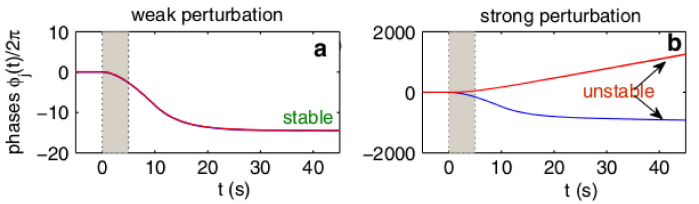

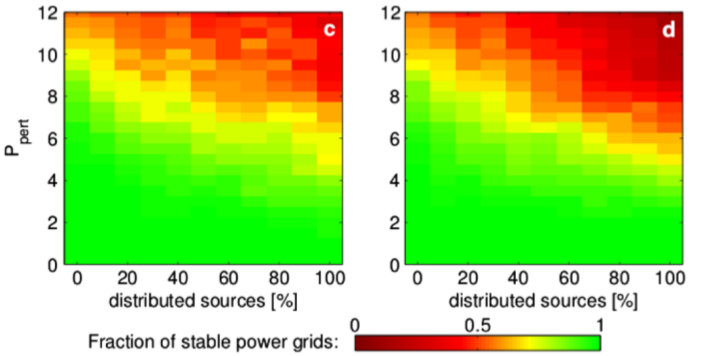

(a) weak and strong (b) perturbation

Turbulent Character of Wind Energy

Wind turbines convert a turbulent wind speed u into a turbulent-like electrical power P. For time scales larger than several minutes, i.e., larger than the regulating time of the control system, power dynamics can be considered to follow adiabatically the wind dynamics with similar -5/3 spectral properties.

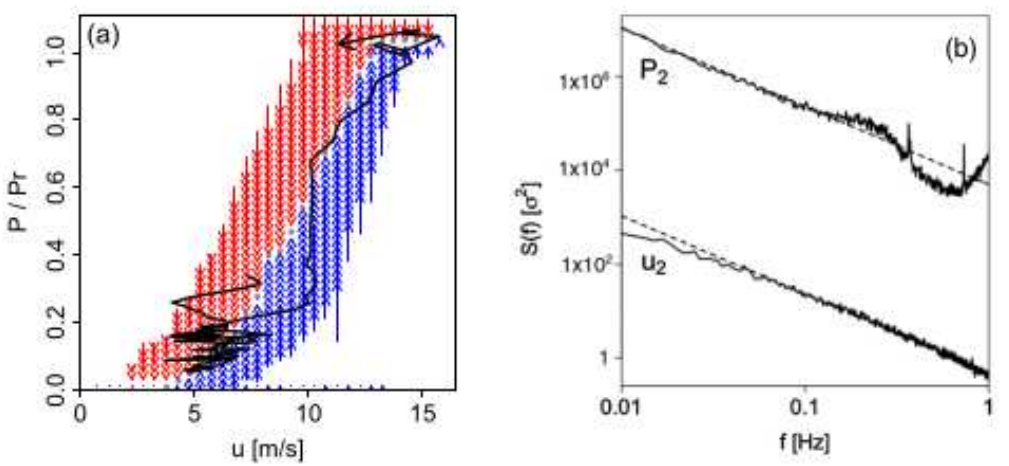

- Trajectory of power output vs wind speed signals for a turbine
- Power spectra of wind speed u^2 and power output P^2

(Milan et al. PRL (2013))

Turbulent Character of Wind Energy

For the smaller time scales, where the control system of the wind conversion systems interacts dynamically with wind fluctuations, the power output has highly intermittent increment PDFs with multifractal scaling close to Kolmogorov's log-normal laws.
The intermittent properties of wind power are maintained on an entire wind farm scale

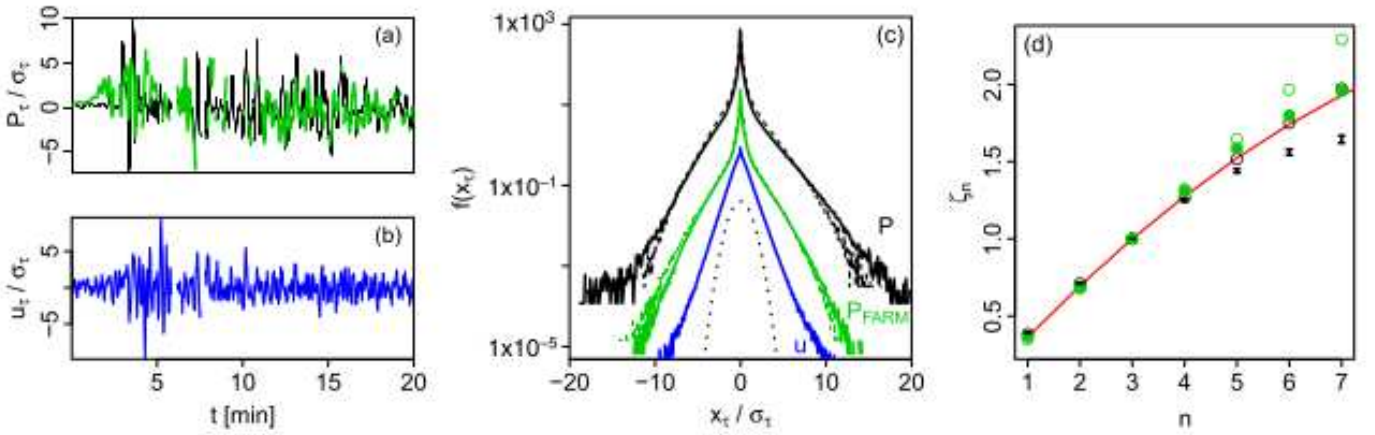

- Normalized increment time series: turbine (black) and farm (green) output, wind speed (blue)
- Increment PDFs for P (upper black), P_{farm} (middle green), and u (lower blue)
- Scaling exponents for P and P_{farm}. Kolmogorov's 1962 model (red line)

(Milan et al. PRL (2013))

Turbulent Character of Solar Energy

The power spectra computed from high frequency time series (with sample rate 1 Hz) of solar irradiance, wind velocity and wind power exhibit a power-law behaviour with an exponent $\sim 5/3$ (Kolmogorov exponent) in the frequency domain 0.001 < f < 0.1 Hz, indicating that they are turbulent-like sources

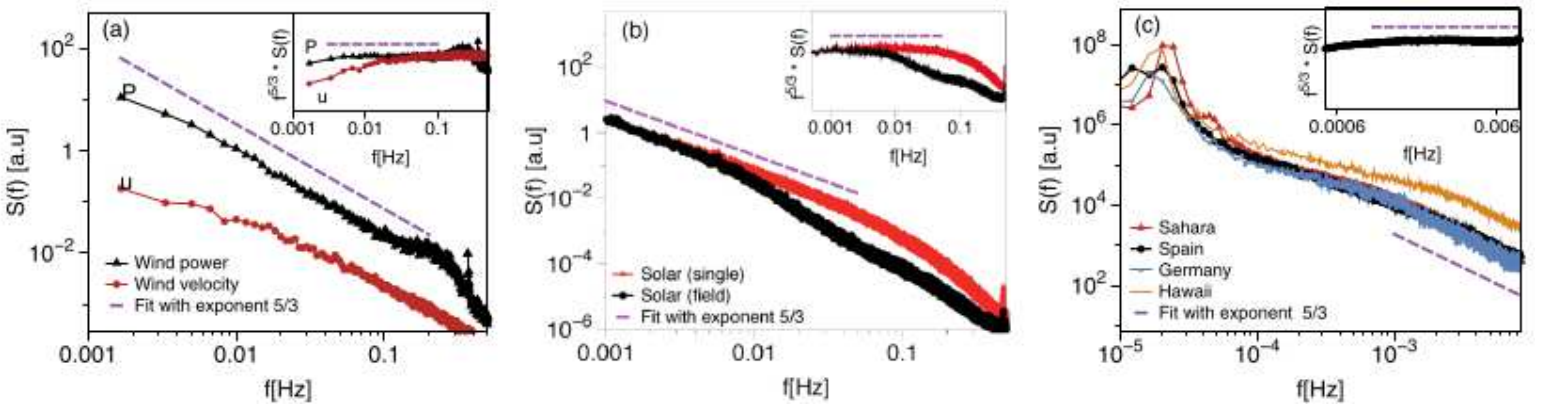

- Power spectra of wind velocity, wind power fluctuations
- Power spectra of irradiance fluctuation for a single site (red) and averaged over 16 sensors (black)
- Power spectra of irradiance fluctuations for minute-averaged solar irradiance

(Anvari et al. New J. Phys. (2016))

Turbulent Character of Solar Energy

Not only the increment PDFs of the single wind turbine and the single solar sensor depart largely from the normal distribution, but also the wind farm and solar field deviate significantly from the Gaussian distribution $\Rightarrow$ extreme events are the normality!

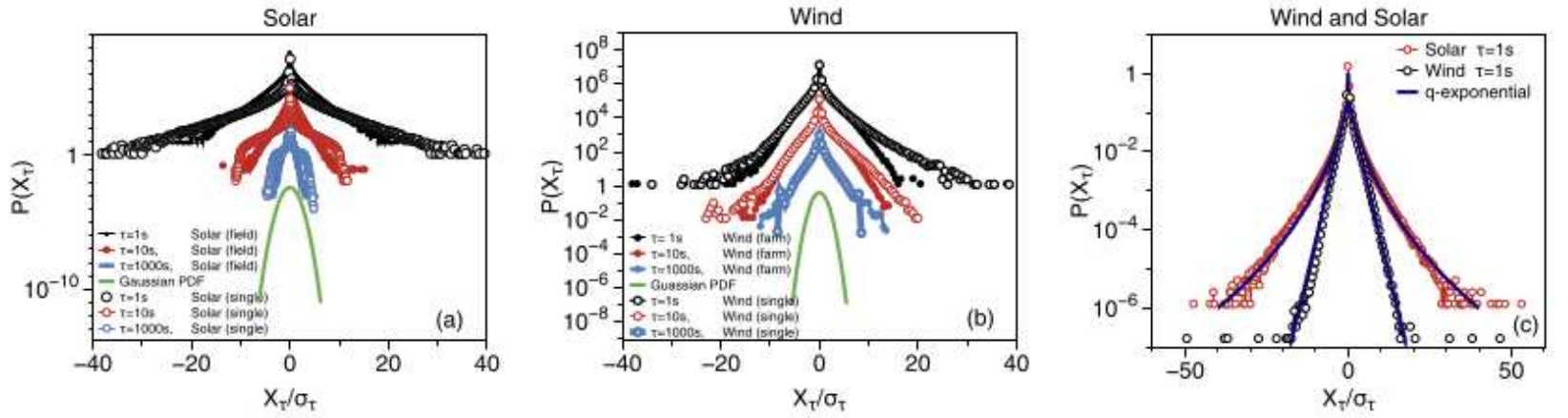

Probability distribution functions (PDF) of increment statistics

- Solar irradiance fluctuations of a single sensor and the whole field
- Wind turbine and wind farm
- Wind and solar power time series

(Anvari et al. New J. Phys. (2016))

Implementing Noise

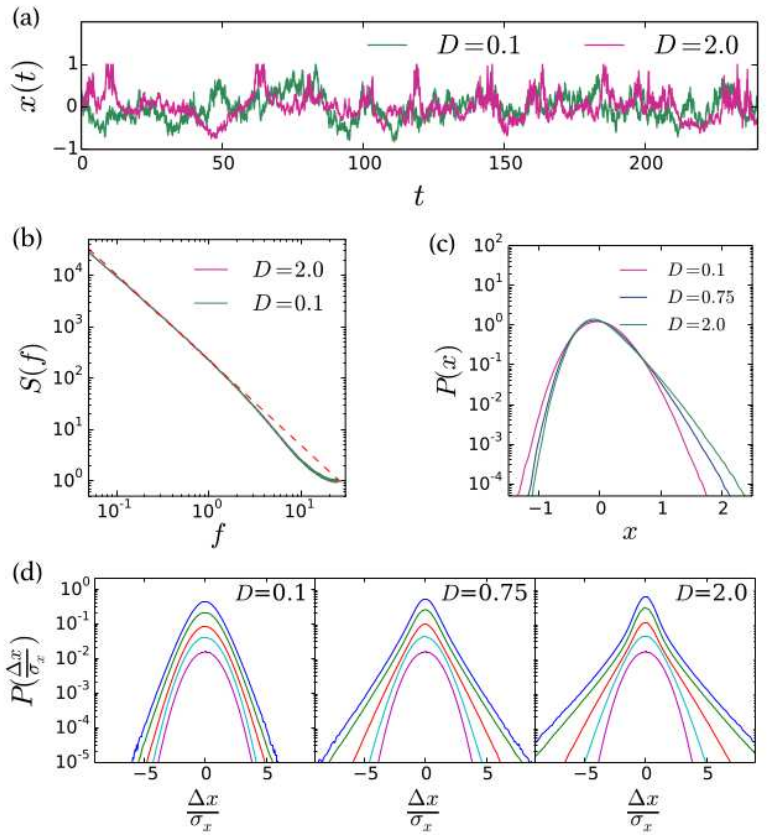

Intermittent power time series are generated by a Langevin-type model

$$\dot{y} = -\gamma y + \Gamma(t), \qquad \dot{x} = x\left(g - \frac{x}{x_0}\right) + \sqrt{Dx^2}y$$

- y colored noise generated by an Ornstein-Uhlenbeck process with correlation time $1/\gamma$
- Γ being δ-correlated Gaussian noise
- D controls the intermittence strength: From D = 0.1 (weakly intermittent, nearly Gaussian) to D = 2.0 (strongly intermittent)

- (a) Time series x(t); (b) Power spectrum S(f)
- (c) PDFs P (x); (d) Normalized PDFs of the increments $\Delta x = x(t) - x(t - \tau)$

(Schmietendorf et al. Eur. Phys. J. B (2017))

Control: Two layer network

Communication infrastructure in a full dynamic description +
Power grid layer : Kuramoto model with inertia

$$m\ddot{\theta}_i(t) = -\dot{\theta}_i(t) + \Omega_i + P_i^c(t) + K\sum^{N} A_{ij}\sin(\theta_j - \theta_i)$$

- i: Node index (=1,...,N)
- θ_i: Phase
- $\dot{\theta}$: Frequency
- m: Mass, inertia constant, m=10
- Ω_i: Inherent frequency $\widehat{=}$ power generation/consumption
- P_i^c: control signal supplied by the communication layer
- A_{ij}: Coupling matrix
- K: Coupling strength

Topology: Italian transmission grid

GENI—Global Energy Network Institute, Map of Italian electricity grid: https://www.geni.org/

- 127 nodes
  34 generators
  93 consumers
- 342 transmission lines
  (220 kV & 380 kV)
- Average connectivity 2.865
- Natural frequencies:
  Ω_{gen}= 93/34
  $\Omega_{load} = -1$

Control: Two layer network

Communication layer:

- Phasor measurement units provide information: local controllers integrated with the generators use the information to calculate a control signal $P_i^c \in \Re$
- The loads are not controlled.
- The control signal can be interpreted as power injection for $P_i^c > 0$ or power absorption for $P_i^c < 0$
- The control is realized using storage devices (batteries) that absorb or inject power to the generator buses [H. Qian et al, IEEE Trans. Power Electron. 26, 886 (2010).]

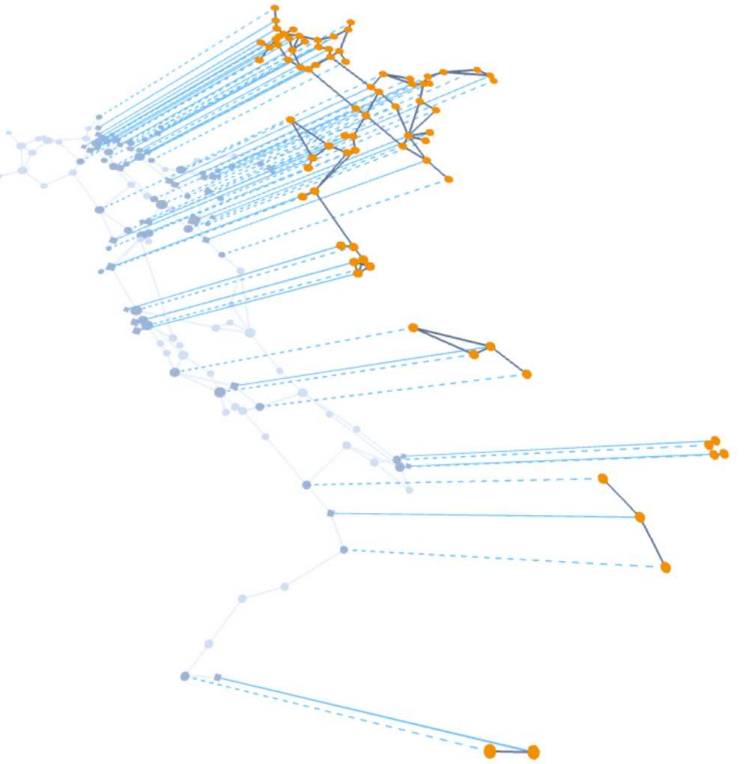

$$\dot{P}_i^c = G_i f_i(c_{i,j}, \{\dot{\theta}_j(t)\})$$

$c_{i,j}$ adjacency matrix of the communication layer

Control: Two layer network

Communication layer:

$$\dot{P}_i^c = G_i f_i(c_{i,j}, \{\dot{\theta}_j(t)\})$$

Control function $f_i(c_{i,j}, \{\dot{\theta}_j(t)\})$:

- Frequency droop control
  $f_i^{diff}(c_{i,j}, \{\dot{\theta}_j(t)\}) = \sum_j^N c_{ij}[\dot{\theta}_j - \dot{\theta}_i]$
  [Giraldo et al, in 52nd IEEE Conf. Decision and Control (2013), 4638]
- Proportional control
  $f_i^{dir}(c_{i,j}, \{\dot{\theta}_j(t)\}) = \frac{-1}{N_i} \sum_j^N c_{ij}\dot{\theta}_j$
- Combined control
  $f_i^{comb}(c_{i,j}, \{\dot{\theta}_j(t)\}) = \sum_j^N c_{ij} \left\{ a[\dot{\theta}_j - \dot{\theta}_i] - b\dot{\theta}_j \right\}$

Control strength G_i: Effective only for generators

- $c_{ij}^{local}, c_{ij}^{global}$

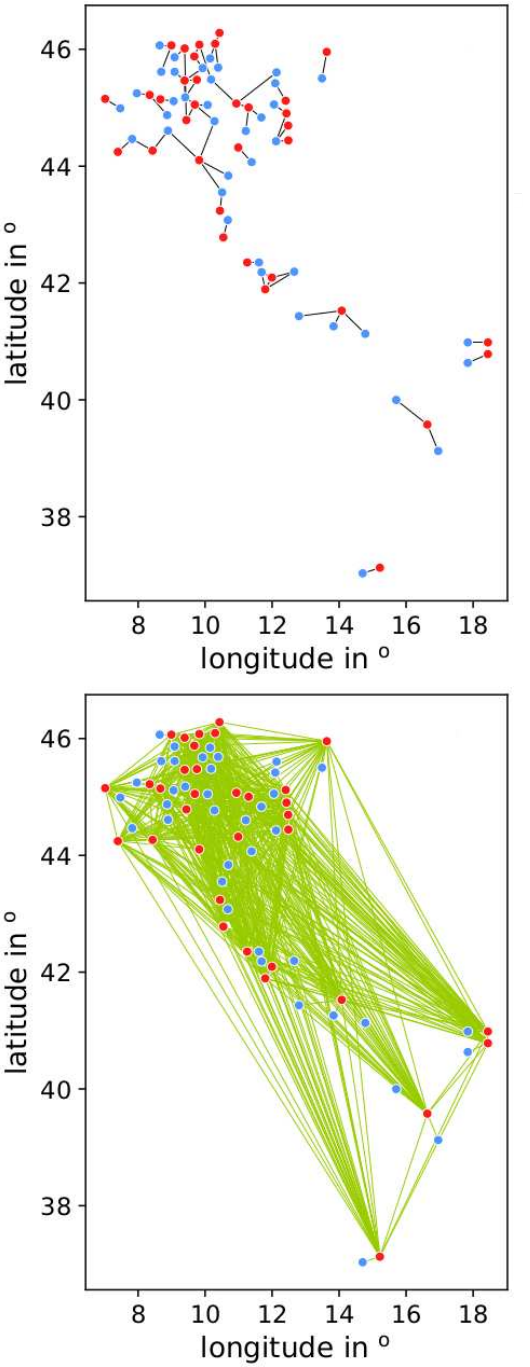

Single node perturbation

Intermittent noise

$$\Omega_i(t) = \Omega_{gen} + \mu x(t)$$

μ= penetration parameter, $x(t)$= intermittent noise series

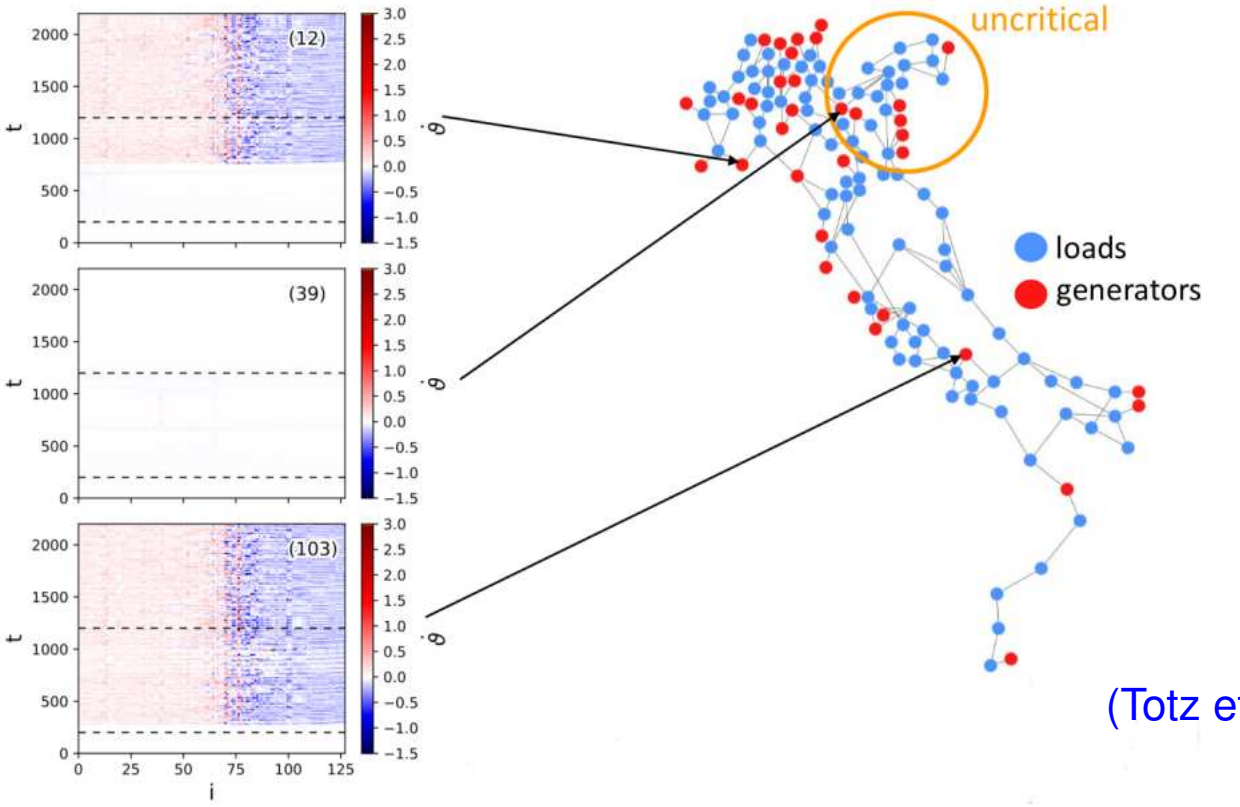

(Totz et al. Phys. Rev E (2020))

Single node perturbation

Intermittent noise

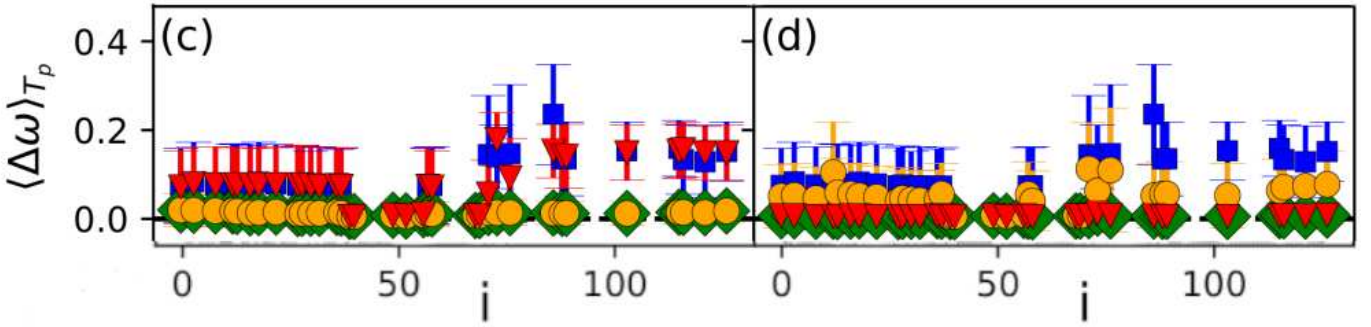

■ no control

▲ $f_i^{diff}(c_{i,j}, \{\dot{\theta}_j(t)\})$ NO

o $f_i^{dir}(c_{i,j}, \{\dot{\theta}_j(t)\})$ OK

♦ $f_i^{comb}(c_{i,j}, \{\dot{\theta}_j(t)\})$ OK

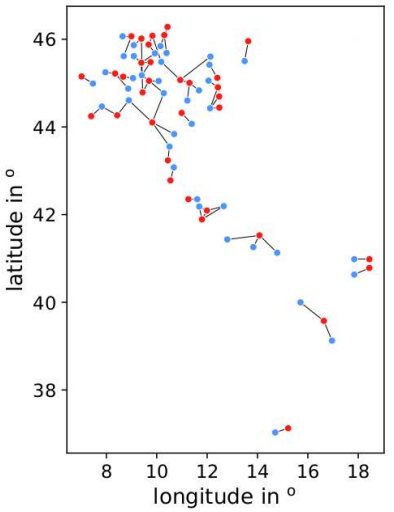

■ no control

▲ $f_i^{diff}(c_{i,j}, \{\dot{\theta}_j(t)\})$ OK

o $f_i^{dir}(c_{i,j}, \{\dot{\theta}_j(t)\})$ NO

♦ $f_i^{comb}(c_{i,j}, \{\dot{\theta}_j(t)\})$ OK

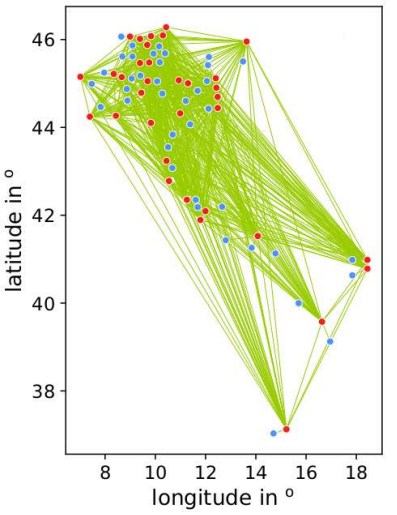

(Totz et al. Phys. Rev E (2020))

Single node perturbation

Disconnecting nodes (generators)

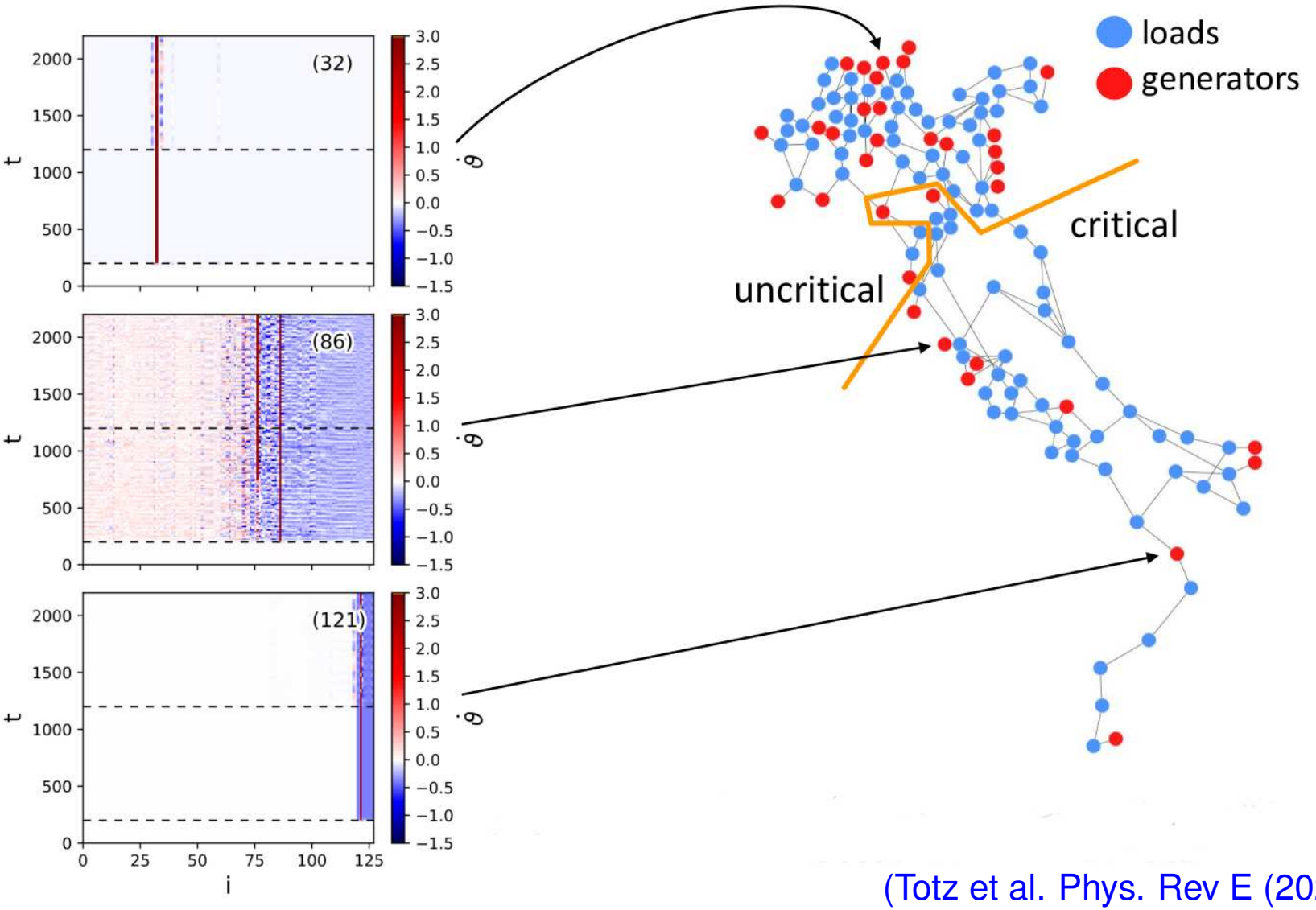

(Totz et al. Phys. Rev E (2020))

Single node perturbation

Disconnecting nodes (generators)

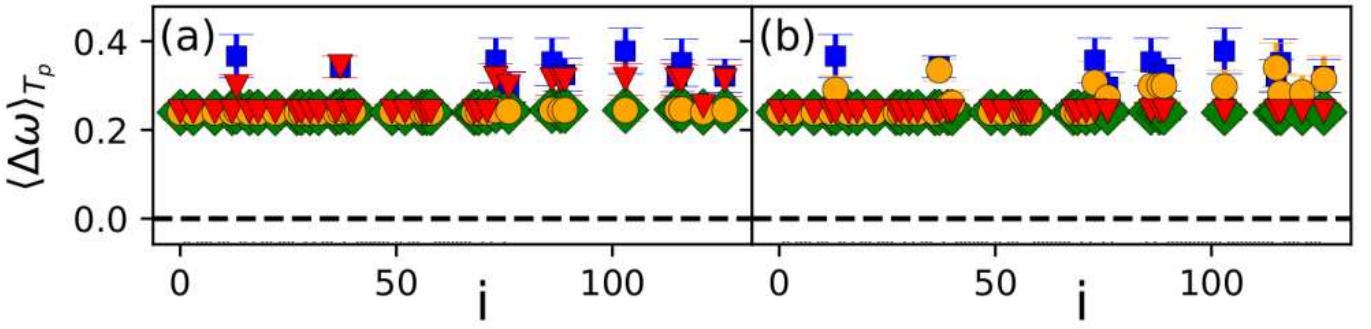

■ no control

▲ $f_i^{diff}(c_{i,j}, \{\dot{\theta}_j(t)\})$ NO

o $f_i^{dir}(c_{i,j}, \{\dot{\theta}_j(t)\})$ OK

♦ $f_i^{comb}(c_{i,j}, \{\dot{\theta}_j(t)\})$ OK

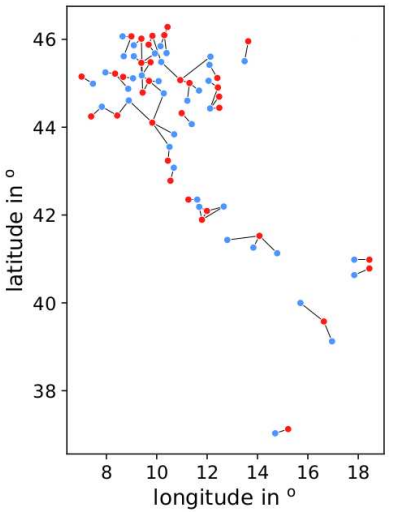

■ no control

▲ $f_i^{diff}(c_{i,j}, \{\dot{\theta}_j(t)\})$ OK

o $f_i^{dir}(c_{i,j}, \{\dot{\theta}_j(t)\})$ NO

♦ $f_i^{comb}(c_{i,j}, \{\dot{\theta}_j(t)\})$ OK

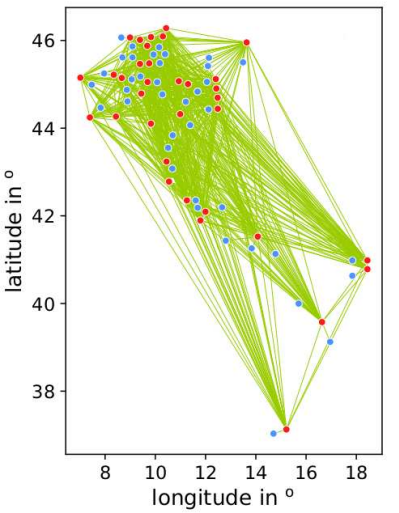

Single node perturbation

Increasing Load Demand

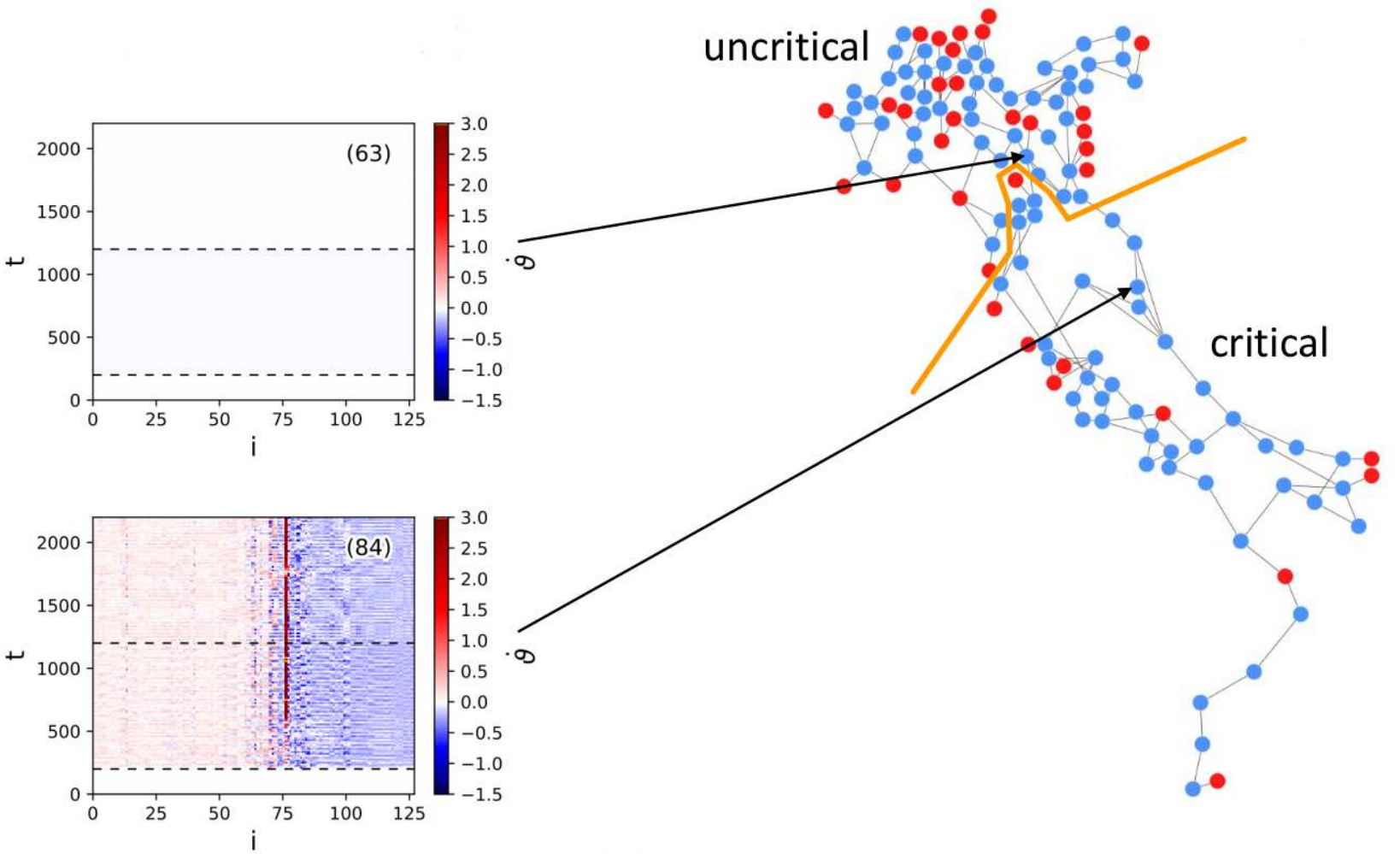

(Totz et al. Phys. Rev E (2020))

Single node perturbation

Increasing Load Demand

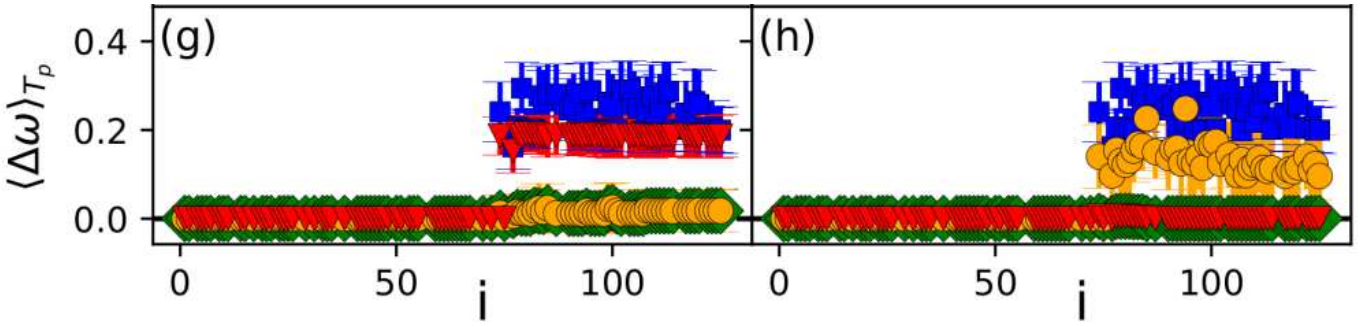

■ no control

▲ $f_i^{diff}(c_{i,j}, \{\dot{\theta}_j(t)\})$ NO

o $f_i^{dir}(c_{i,j}, \{\dot{\theta}_j(t)\})$ OK

♦ $f_i^{comb}(c_{i,j}, \{\dot{\theta}_j(t)\})$ OK

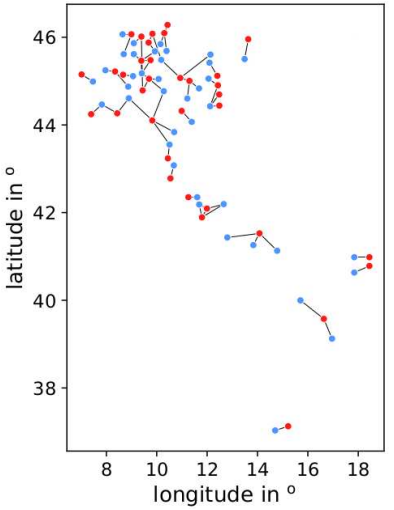

■ no control

▲ $f_i^{diff}(c_{i,j}, \{\dot{\theta}_j(t)\})$ OK

o $f_i^{dir}(c_{i,j}, \{\dot{\theta}_j(t)\})$ NO

♦ $f_i^{comb}(c_{i,j}, \{\dot{\theta}_j(t)\})$ OK

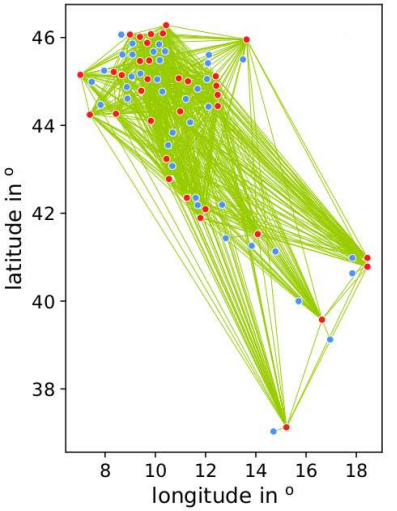

Italian High Voltage Power Grid

- We do not observe any hysteretic behavior or multistability down to $K = 9$
- For smaller coupling an intricate behavior is observable depending on initial conditions
- Generators and consumers compete in order to oscillates at different frequencies
- The local architecture favours a splitting based on the proximity of the oscillators
- Several small whirling clusters appear characterized by different phase velocities
- The irregular oscillations in $r(t)$ reflect quasi-periodic motions

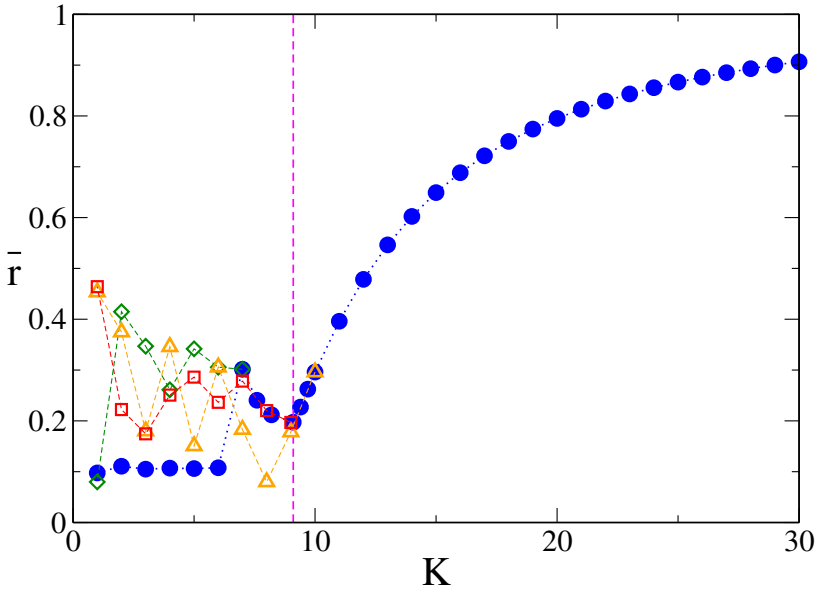

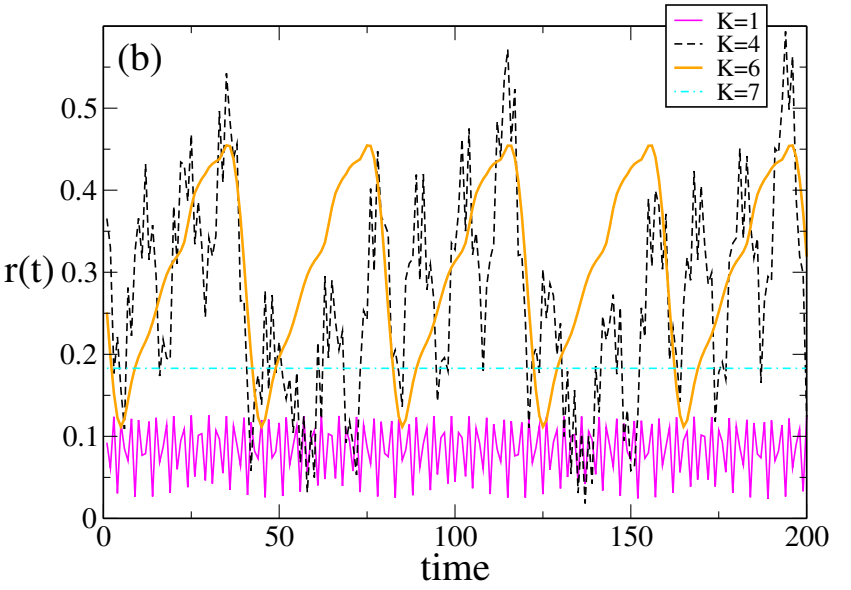

Italian High Voltage Power Grid

By following Protocol II

- the system stays in one cluster up to $K = 7$
- at $K = 6$ wide oscillations emerge in $r(t)$ due to the locked clusters that have been splitted in two (is this also the origin for the emergent multistability?)
- By lowering further K several whirling small clusters appear and r becomes irregular

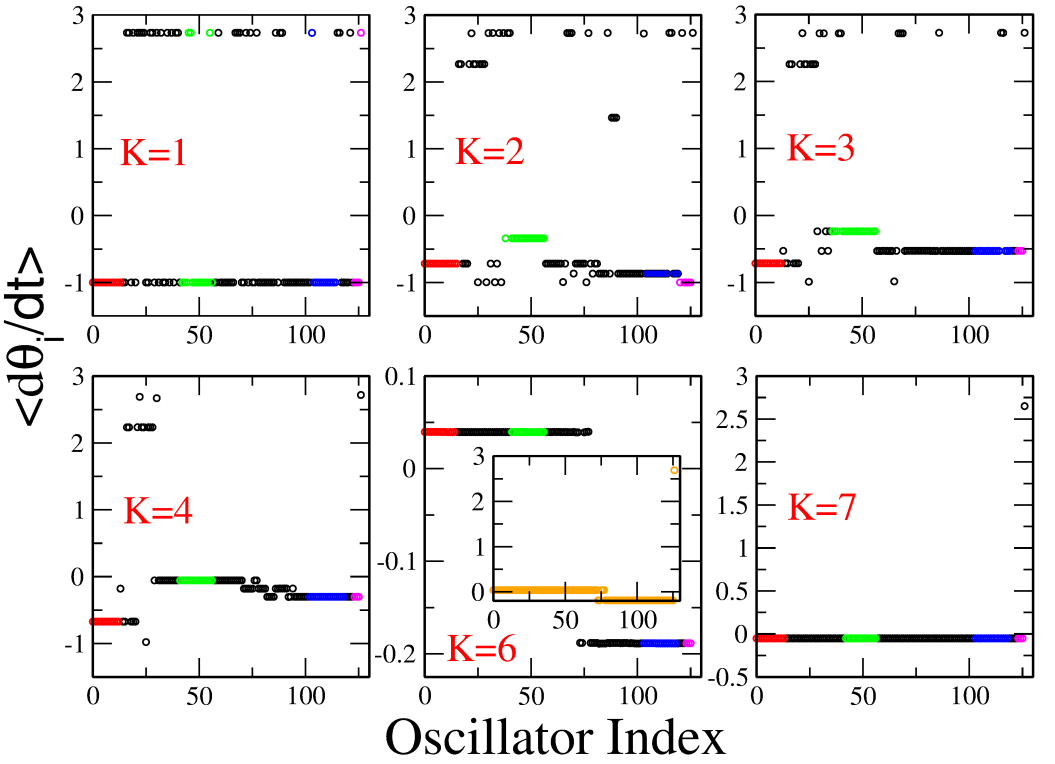

(Olmi et al. Phys. Rev E (2014))

References

B. Ermentrout, Journal of Mathematical Biology 29 , 571 (1991)

EE. Hanson, Cellular Pacemakers, ed. D.O. Carpenter, Vol. 2 (Wiley, New York, 1982) pp. 81-100

S. H. Strogatz, Nonlinear Dynamics And Chaos: With Applications To Physics, Biology, Chemistry, And Engineering, 1st Edition, Westview Press (1994)

B. R. Trees, V. Saranathan, D. Stroud, Phys Rev E 71 (1) (2005) 016215

G. Filatrella, A. H. Nielsen, N. F. Pedersen, Eur Phys J B 61 (4), 485-491 (2008)

H. A. Tanaka, A. J. Lichtenberg, S. Oishi, Phys Rev Lett 78 (11) (1997) 2104-2107 (1997)

S. Olmi, A. Navas, S. Boccaletti, A. Torcini, Phys Rev E 90 (4), 042905 (2014)

M. Rohden, A. Sorge, M. Timme, D. Witthaut, Phys Rev Lett 109 (6), 064101 (2012)

P. Milan, M. Wächter, J. Peinke, Physical review letters 110 (13), 138701 (2013)

M. Anvari, G. Lohmann, M. Wächter, P. Milan, E. Lorenz, D. Heinemann, M. Tabar, J. Peinke, New Journal of Physics 18 (6), 063027 (2016)

K. Schmietendorf, J. Peinke, O. Kamps, Eur Phys J B 90 (11), 1-6 (2017).

C. Totz, S. Olmi, E. Schöll, Phys Rev E 102 (2), 022311 (2020).

Linear Stability Analysis of the Asynchronous State

- Tool: nonlinear Fokker-Planck formulation for the evolution of the single oscillator distribution $\rho(\theta, \dot{\theta}, \Omega, t)$ for coupled oscillators with inertia and noise
- Critical coupling K_1^{MF} for an unimodal frequency distribution $g(\Omega)$ with width Δ

$$\frac{1}{K_1^{MF}} = \frac{\pi g(0)}{2} - \frac{m}{2}\int_{-\infty}^{\infty} \frac{g(\Omega)d\Omega}{1+m^2\Omega^2}$$

- If $g(\Omega)$ is Lorentzian $\Rightarrow K_1^{MF} = 2\Delta(1+m\Delta)$
- If $g(\Omega)$ is Gaussian
  - the zero mass limit gives

$$K_1^{MF} = 2\Delta\sqrt{\frac{2}{\pi}}\left\{1+\sqrt{\frac{2}{\pi}}m\Delta+\frac{2}{\pi}m^2\Delta^2+\sqrt{\left(\frac{2}{\pi}\right)^3-\frac{2}{\pi}}m^3\Delta^3\right\}+\mathcal{O}(m^4\Delta^4)$$

  - The limit $m\Delta \to \infty$ gives $K_1^{MF} \propto 2m\Delta^2$

(Acebron et al. PRE (2000); Gupta et al. (PRE 2014))

Finite size effects for K_1^c

If $g(\Omega)$ is an unimodal, symmetric distribution with zero mean

$$\frac{1}{K_1^{MF}} = \frac{\pi g(0)}{2} - \frac{m}{2}\int_{-\infty}^{\infty} \frac{g(\Omega)d\Omega}{1+m^2\Omega^2}$$

How to identify the scaling law ruling the approach of $K_1^c(N)$ to its mean-field value for increasing system sizes?

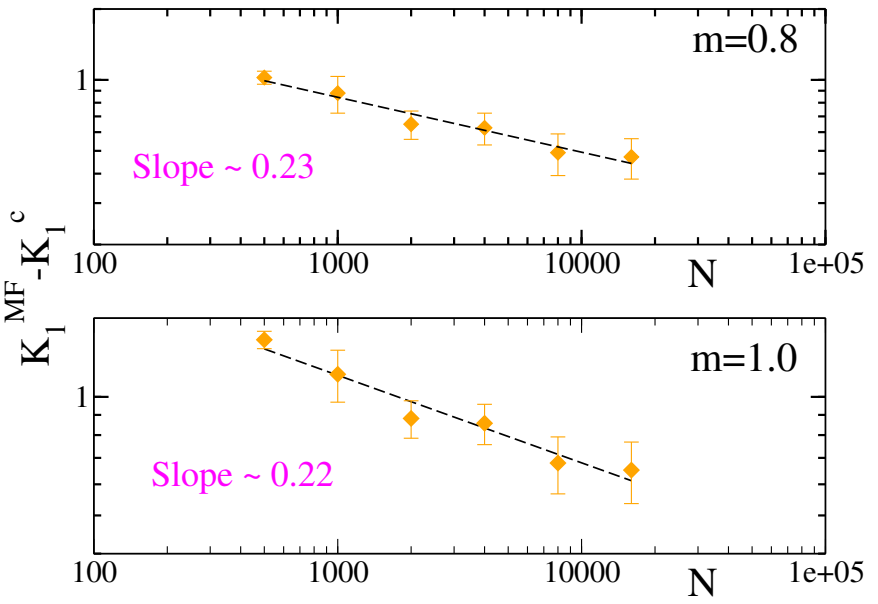

Power-law scaling with the system size N for fixed mass

$$K_1^{MF} - K_1^c(N) \propto N^{-1/5}$$

$\Rightarrow$ this is true for sufficently low masses

Mean Field Theory with Noise (Acebrón, Spigler (2008))

ξ_i independent sources of Gaussian white noise

$$\begin{aligned} \dot{\theta}_i &= \nu_i \\ m\dot{\nu}_i &= -\nu_i + \Omega_i + Kr\sin(\phi - \theta_i) + \xi_i \end{aligned}$$

with $< \xi_i >= 0$ and $< \xi_i(t)\xi_j(t) >= 2D\delta_{ij}\delta(t-s)$

- Continuum limit (continuity equation for $\rho(\theta, \nu, \Omega, t)$)

$$\frac{\partial \rho}{\partial t} = \frac{D}{m^2}\frac{\partial^2 \varrho}{\partial \nu^2} - \frac{1}{m}\frac{\partial}{\partial \nu}\left[(-\nu + \Omega + Kr\sin(\phi - \theta))\rho\right] - \nu\frac{\partial \rho}{\partial \theta}$$

- Normalization $\int_{-\infty}^{\infty}\int_{-\pi}^{\pi}\rho(\theta, \nu, \Omega, 0)d\theta d\nu = 1$
- Identical oscillators $g(\Omega) = \delta(\Omega)$

Stationary solution $\rho(\theta, \nu) = \chi(\theta)\eta(\nu)$

$\Rightarrow$ It is possible to find frequency and phase distribution from the continuity equation

$\Rightarrow$ K_1^{MF} turns out to be independent of the inertia

Mean Field Theory with Noise

Via averaging the velocity $\nu(t)$ in the long-time limit, the Fokker-Planck equation for the probability distribution $\rho(\theta, \nu, \Omega, t)$ reduces to the Smoluchowski equation

$$\frac{\partial \rho(\theta,t)}{\partial t} = \frac{\partial}{\partial \theta}\left[\left(\frac{\partial V(\theta)}{\partial \theta} + D\frac{\partial \rho(\theta)}{\partial \theta}\right)\left(1 + m\frac{\partial^2 V(\theta)}{\partial \theta^2}\right)\right]$$

with the potential $V(\theta) = -Kr\cos(\theta) - \Omega\theta$. For $D = 0$, the stationary state solution gives

$$r = \left(\tfrac{\pi}{2} - \tfrac{m}{2}\right) g(0)Kr + \tfrac{4}{3}mg(0)(Kr)^2 + \tfrac{\pi}{16}g''(0)(Kr)^3 + \mathcal{O}(Kr)^4$$

- Drifting and locked oscillators are both contributing to the phase coherence
- The quadratic term $(Kr)^2$ induces hysteresis in the bifurcation diagram
- The hysteresis is reduced with noise
- The critical coupling strength increases monotonically with the increase of D
- The response of phase velocity to external driving is enhanced by a certain amount of noise

(Hong et al. (1999); Bonilla (2000); Hong, Choi (2000))

Bestiary

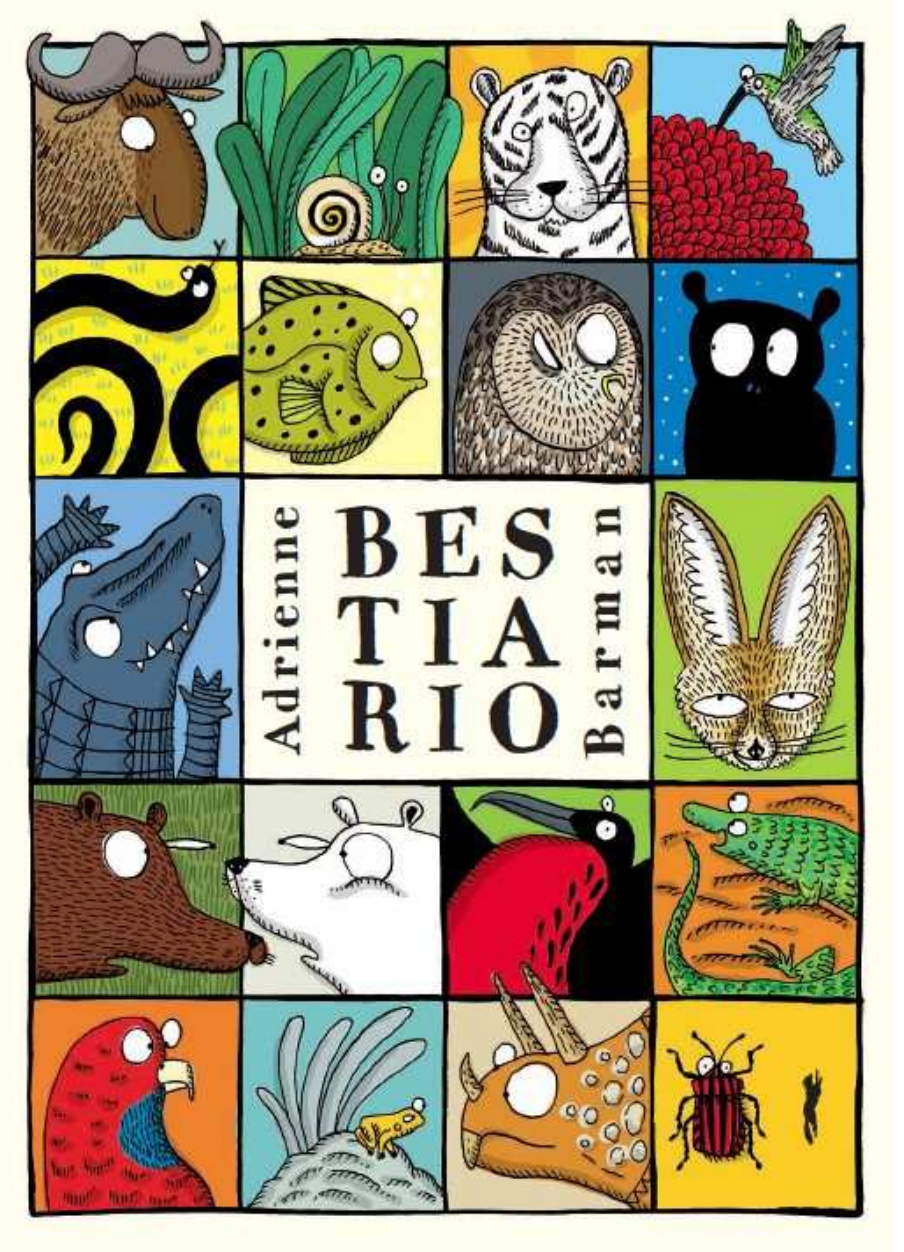

Simulations: Noise + Bimodal Frequency Distribution

- Globally coupled network with Bimodal Gaussian frequency distribution
- W_h width of the hysteretic loop, $m = 8$

$$m\ddot{\theta}_i + \dot{\theta}_i = \Omega_i + \frac{K}{N}\sum_j \sin(\theta_j - \theta_i) + \sqrt{2D}\xi_i$$

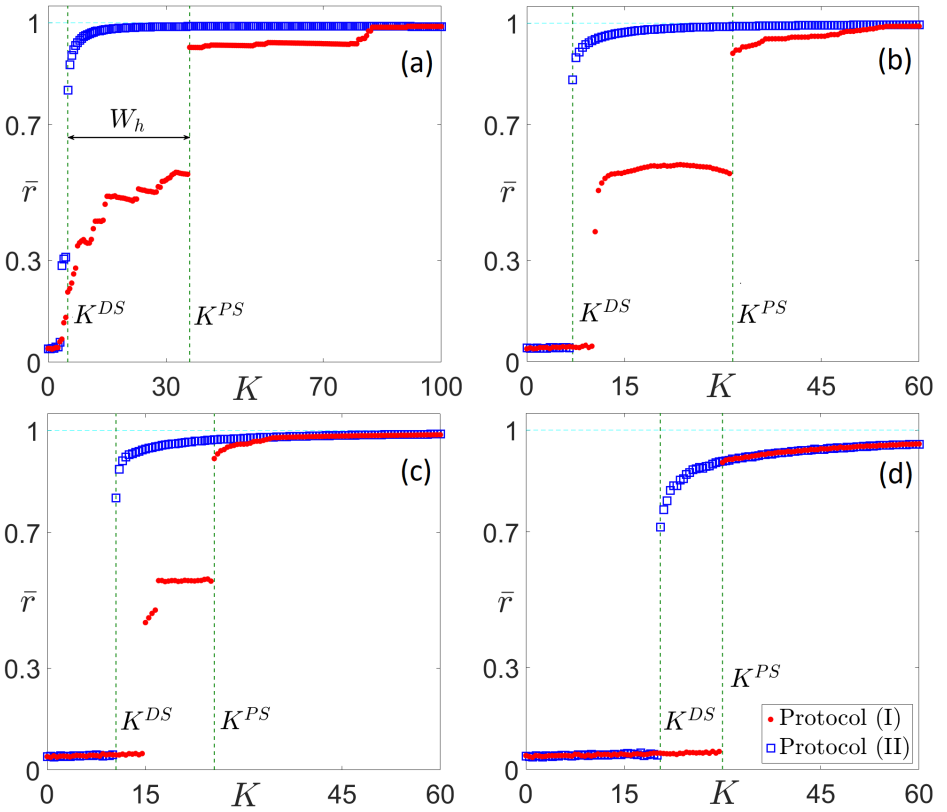

(a) D=0; b) 2D = 9;
(c) 2D = 15; (d) 2D = 30

- Hysteresis is reduced with noise
- Intermediate states are suppressed

(Tumash et al. (2018))

Simulations: Noise + Bimodal Frequency Distribution

$D = 0$, $m = 8$

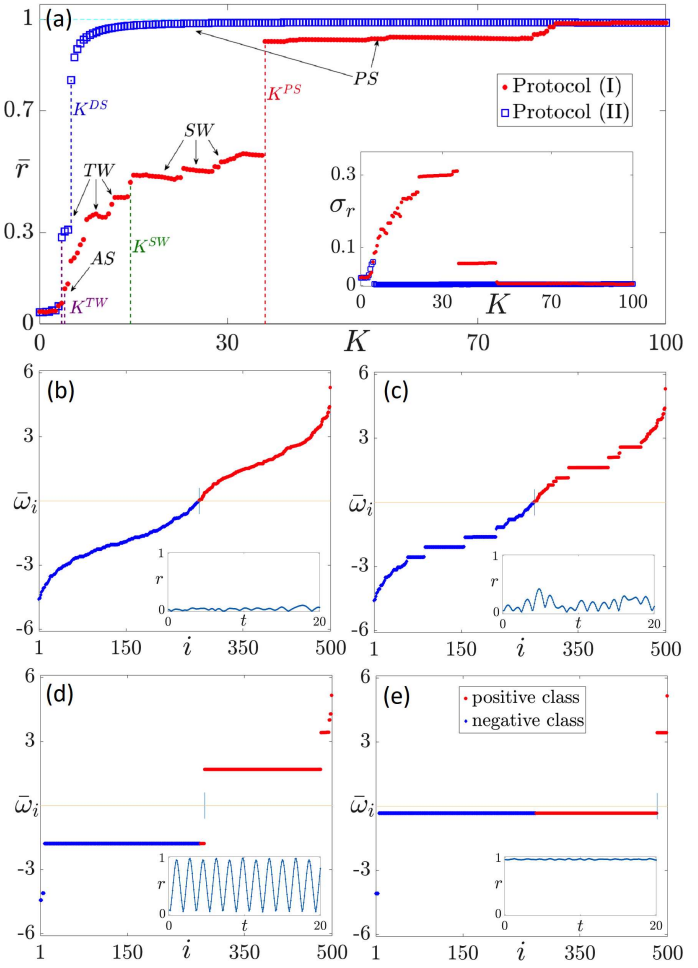

(a) $m = 1$, (b) $m = 30$

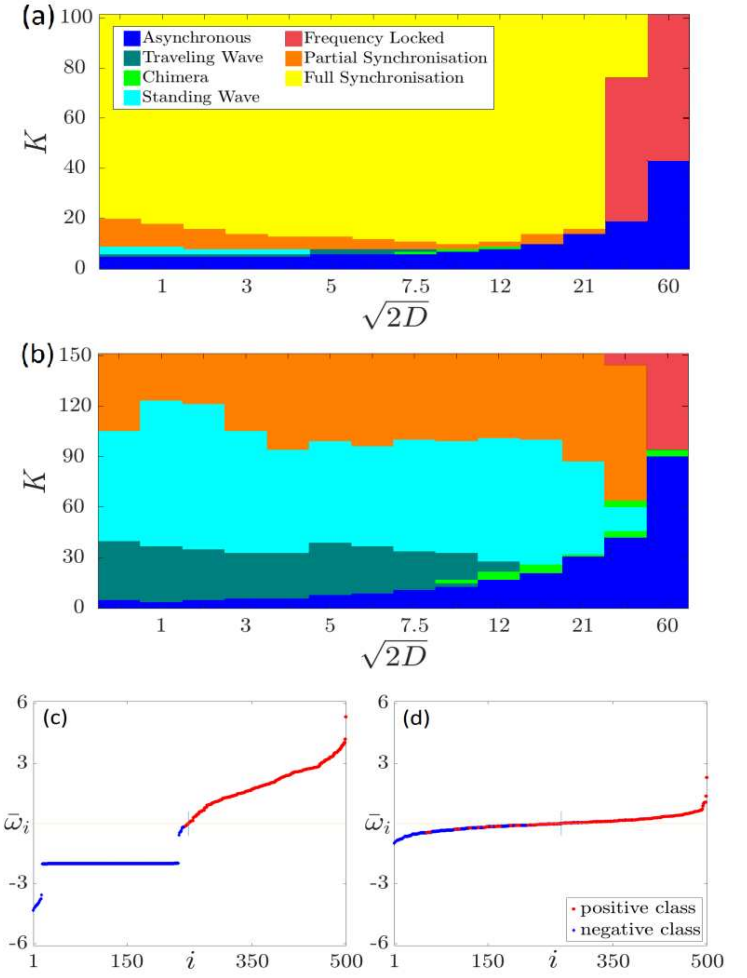

(Tumash et al. (2018))

Further works: diluted network + $g(\Omega)$ unimodal

- Constraint 1 : the random matrix is symmetric
- Constraint 2 : the in-degree is constant and equal to N_c

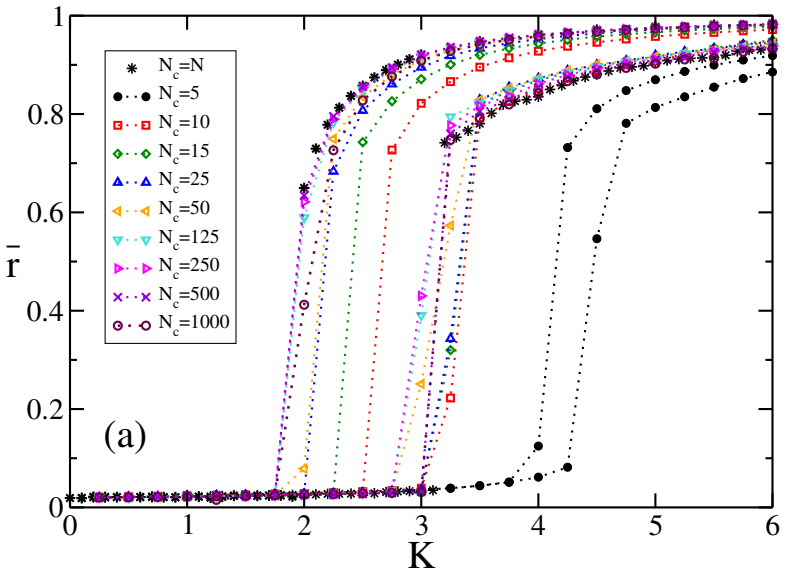

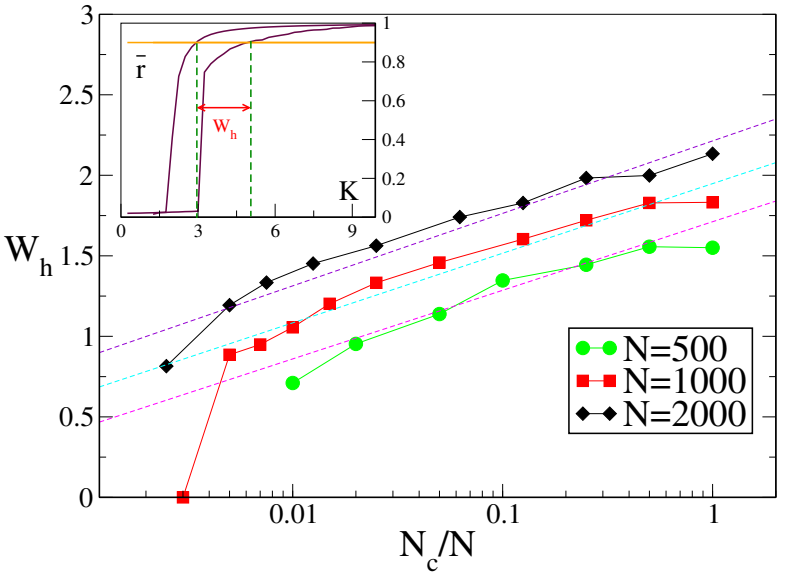

- Diluted or fully coupled systems (whenever the coupling is properly rescaled with the in-degree) display the same phase-diagram
- For very small connectivities the transition from hysteretic becomes continuous
- By increasing the system size the transition will stay hysteretic for extremely small percentages of connected (incoming) links

Further works: $g(\Omega)$ bimodal

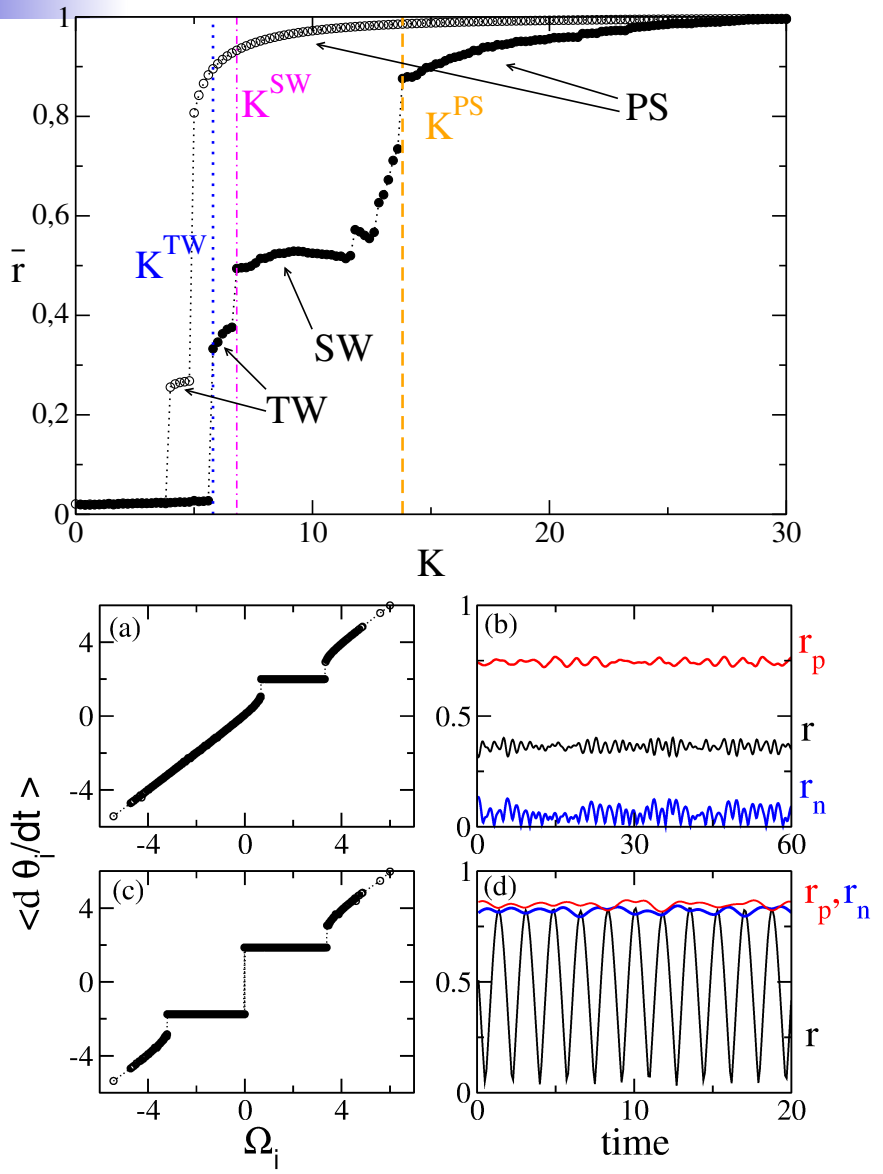

Globally coupled network

- Traveling Wave (TW): a single cluster of oscillators, drifting together with a velocity Ω_0
- Standing Wave (SW): two clusters of drifting oscillators with symmetric opposite velocities $\pm\Omega_0$
- Partially Synchronized state (PS): a cluster of locked rotators with zero average velocity

(Olmi, Torcini (2016))

Further works: diluted network + $g(\Omega)$ bimodal

$p = 0.25$

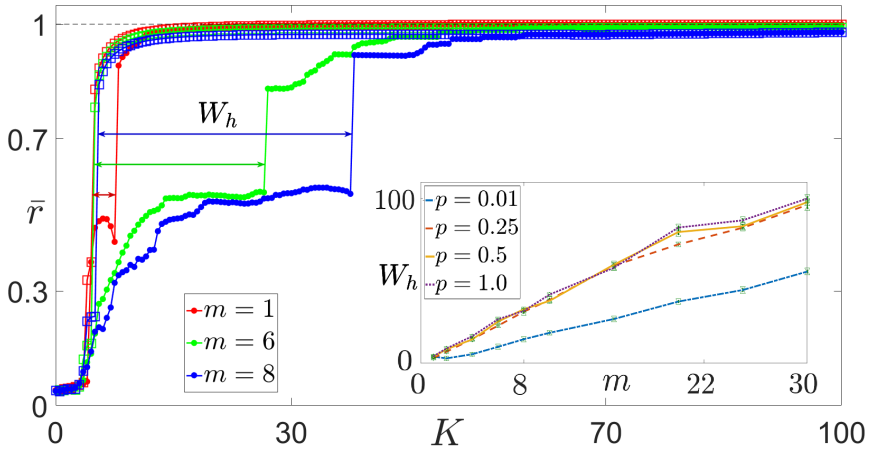

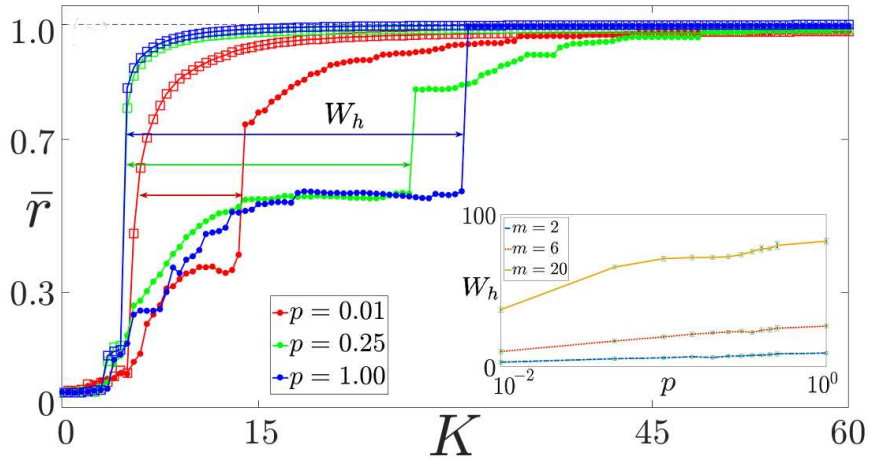

$m = 6$

- For bigger masses, larger values of critical coupling are required to reach synchronization
- $N_c = pN$
- The hysteretic loop decreases as the network topology becomes more sparse

(Tumash et al. (2018))

Further works: frequency-degree correlation

Ω_i proportional to its degree with zero mean (so that $\sum_i \Omega_i = 0$) : $\Omega_i = B(k_i - < k >)$

$$m\ddot{\theta}_i + \dot{\theta}_i = B(k_i - < k >) + \lambda \sum_j A_{i,j} \sin(\theta_j - \theta_i)$$

Average frequency $< \omega_k >$ of nodes with the same degree k:

$$< \omega_k >= \sum_{[i|k_i=k]} < \dot{\theta}_i >_t /(NP(k))$$

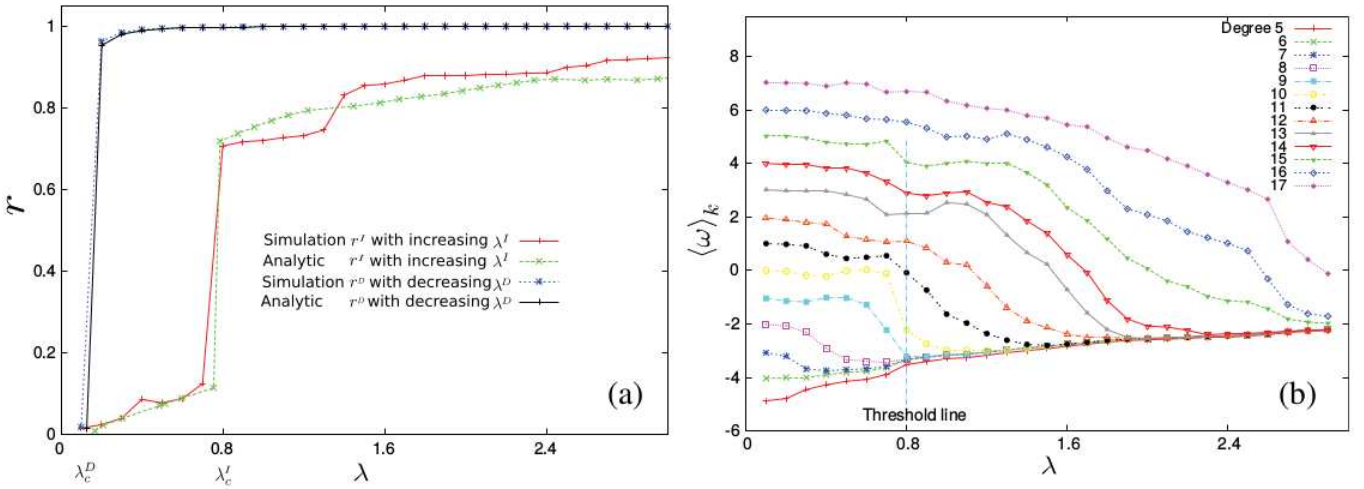

- Oscillators join the synchronous component grouped into clusters of nodes with the same degree
- Small degree nodes synchronize first (cluster explosive synchronization)

(Ji et al. (2013) – extension of TLO theory)

Josephson Junctions

- The Josephson effect is the phenomenon of supercurrent, a current that flows indefinitely long without any voltage applied, through a Josephson junction (JJ)
- A JJ consists of two or more superconductors coupled by a weak link, which can consist of a thin insulating barrier, a short section of non-superconducting metal, or a physical constriction that weakens the superconductivity at the point of contact
- The Josephson effect is an example of a macroscopic quantum phenomenon, predicted by Brian David Josephson in 1962 (Josephson (1962))
- The DC Josephson effect had been seen in experiments prior to 1962, but had been attributed to "super-shorts" or breaches in the insulating barrier
- The first paper to claim the discovery of Josephson's effect, and to make the requisite experimental checks, was that of (Anderson and Rowell (1963))
- Before JJ, it was only known that normal, non-superconducting electrons can flow through an insulating barrier (quantum tunneling). Josephson first predicted the tunneling of superconducting Cooper pairs (Nobel Prize in Physics 1973).

A locally coupled Kuramoto model with inertia can be derived from a coupled resistively and capacitively shunted junction eqs for an underdamped ladder with periodic boundary conditions (Trees et al. (2005)): good agreements are achieved for phase and frequency synchronization

References

H. D. Chiang, BCU Methodologies, and Applications, John Wiley & Sons (2011)

M. Levi, F. C. Hoppensteadt, W. L. Miranker, Quarterly of Applied Mathematics 36.2, 167-198 (1978)

S. Gupta, A. Campa, S. Ruffo, Phys Rev E 89 (2) 022123 (2014)

J. A. Acebrón, L. L. Bonilla, R. Spigler, Phys Rev E 62 (3) 3437-3454 (2000)

J. A. Acebrón, R. Spigler, Phys Rev Lett 81 (11) 2229-2232 (2008)

H. Hong, M. Choi, B. Yoon, K. Park, K. Soh, Journal of Physics A: Mathematical and General 32 (1) L9 (1999)

L. L. Bonilla, Phys Rev E 62 (4), 4862-4868 (2000)

H. Hong, M. Y. Choi, Phys Rev E 62 (5) (2000) 6462-6468

L. Tumash, S. Olmi, E. Schöll, EPL 123, 20001 (2018)

S. Olmi, A. Torcini, in Control of Self-Organizing Nonlinear Systems, 25-45 (2016)

P. Ji, T. K. D. Peron, P. J. Menck, F. A. Rodrigues, J. Kurths, Phys Rev Lett 110 (21), 218701 (2013)

B. D. Josephson, Physics letters 1 (7): 251-253 (1962)

P. W. Anderson, J. M. Rowell, Phys Rev Lett 10 (6): 230 (1963)

Extension of the Mean Field Theory

In principle one could fix the discriminating frequency to some arbitrary value Ω_0 and solve self-consistently

$$r = r_L + r_D$$

$$r_L^{I,II} = Kr \int_{-\theta_0}^{\theta_0} \cos^2\theta g(Kr\sin\theta)d\theta \quad r_D^{I,II} \simeq -mKr \int_{-\Omega_0}^{\infty} \frac{1}{(m\Omega)^3} g(\Omega)d\Omega$$

This amounts to obtain a solution $r^0 = r^0(K, \Omega_0)$ by solving

$$\int_{-\theta_0}^{\theta_0} \cos^2\theta g(Kr^0\sin\theta)d\theta - m\int_{-\Omega_0}^{\infty} \frac{1}{(m\Omega)^3} g(\Omega)d\Omega = \frac{1}{K}$$

with $\theta_0 = \sin^{-1}(\Omega_0/Kr^0)$. The solution exists if $\Omega_0 < \Omega_D = Kr^0$.

$\Rightarrow$ A portion of the (K, r) plane delimited by the curve $r^{II}(K)$ is filled with the curves $r^0(K)$ obtained for different Ω_0 values.

Drifting Clusters (Olmi et al. (2014))

- The amplitude of the oscillations of $r(t)$ and the number of oscillators in the drifting clusters N_{DC} correlates in a linear manner
- The oscillations in $r(t)$ are induced by the presence of large secondary clusters characterized by finite whirling velocities
- At smaller masses oscillations are present, but reduced in amplitude. Oscillations are due to finite size effects since no clusters of drifting oscillators are observed

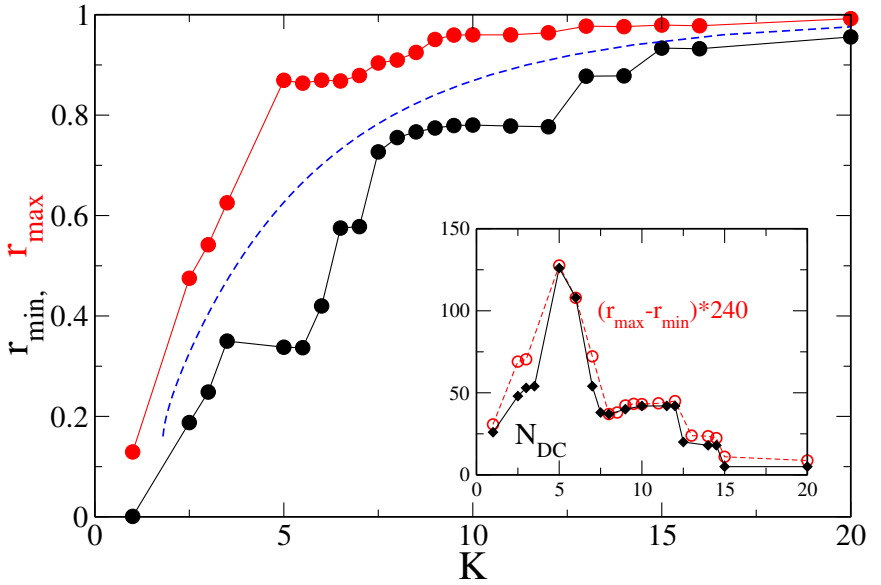

- Blue dashed line $\Rightarrow$ estimated mean field value r^I by Tanaka et al. (1997)
- The mean field theory captures the average increase of the order parameter but it does not foresee the oscillations

Dependence On the Mass K_1^c

- K_1^c increases with m up to a maximal value and than decreases at larger masses
- by increasing N K_1^c increases and the position of the maximum shifts to larger masses (finite size effects)

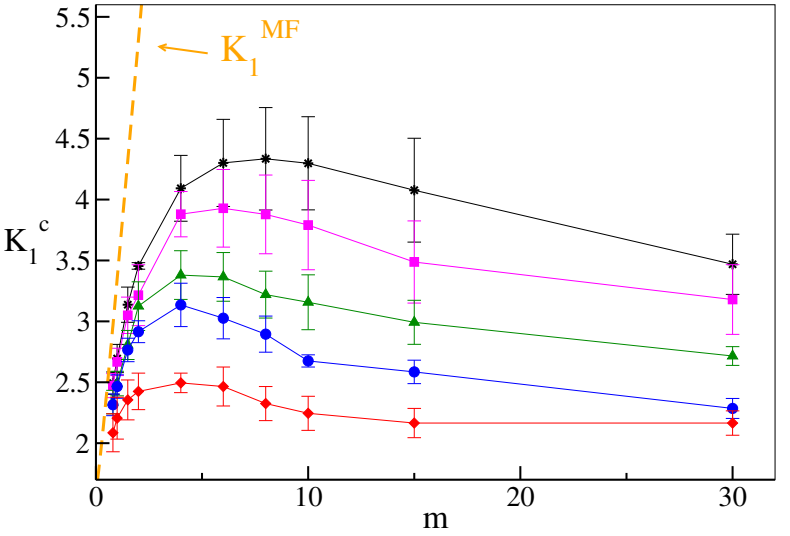

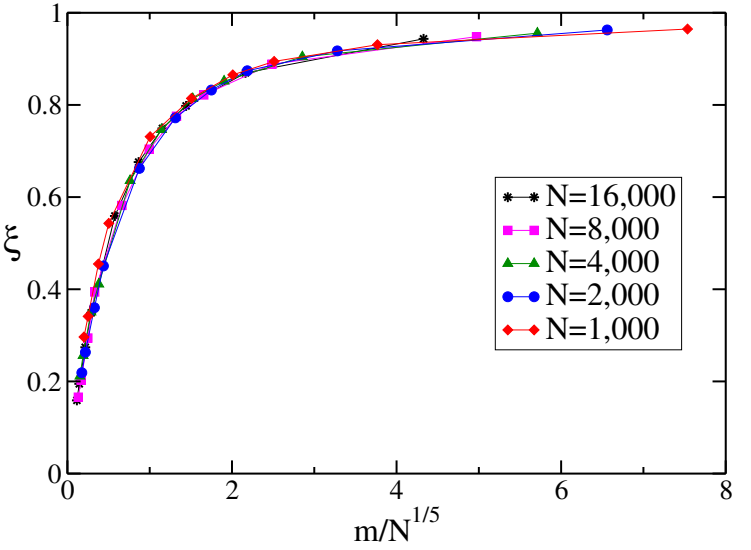

The following general scaling seems to apply

$$\xi \equiv \frac{K_1^{MF} - K_1^c(m,N)}{K_1^{MF}} = G\left(\frac{m}{N^{1/5}}\right) \quad \text{where } K_1^{MF} \propto 2m \text{ for } m > 1$$

Dependence On the Mass K_2^c

The TLO approach fails to reproduce the critical coupling for the transition from asynchronous to synchronous state (i.e., K_1^c), however it gives a good estimate of the return curve obtained with protocol II from the synchronized to the aynchronous regime

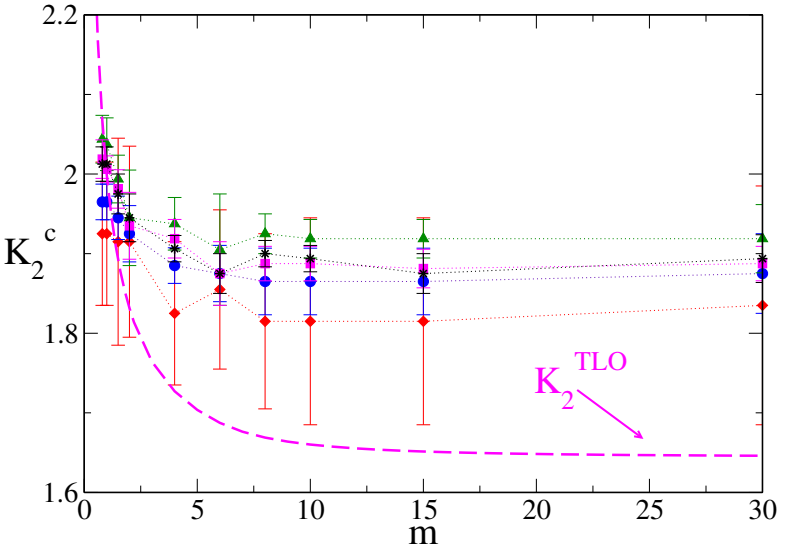

- K_2^c initially decreases with m then saturates, limited variations with the size N
- K_2^{TLO} is the minimal coupling associated to a partially synchronized state given by TLO approach for protocol II
- K_2^{TLO} exhibits the same behaviour as K_2^c, however it slightly understimates the asymptotic value (see the scale)

Further works: diluted network

- The TLO mean field theory still gives reasonable results (70% of broken links)
- All the states between the synchronization curves obtained following Protocol I and II are reachable and stable

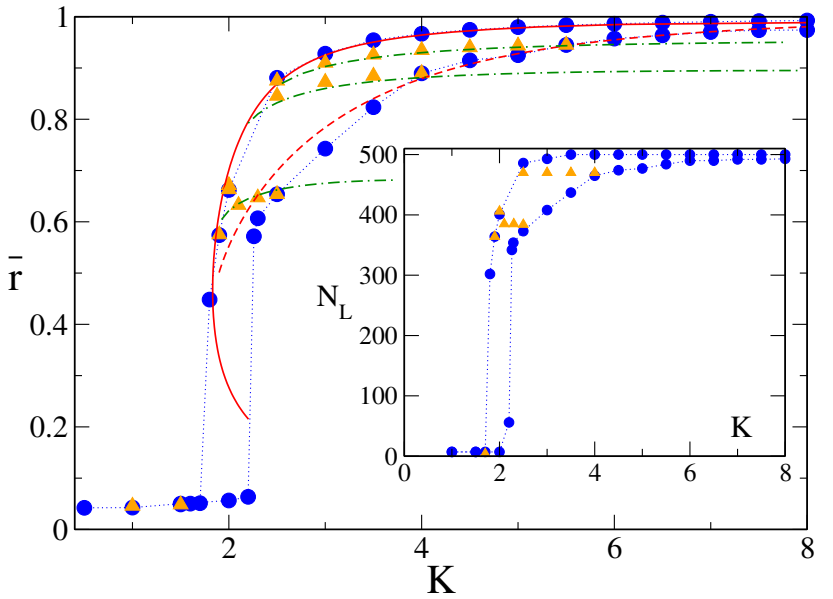

- These states, located in the region between the synchronization curves, are characterized by a frozen cluster structure, composed by a constant N_L
- The generalized mean-field solution $r^0(K, \Omega_0)$ is able to well reproduce the numerically obtained paths connecting the synchronization curves (I) and (II)

Further works: $g(\Omega)$ bimodal Finite size effects

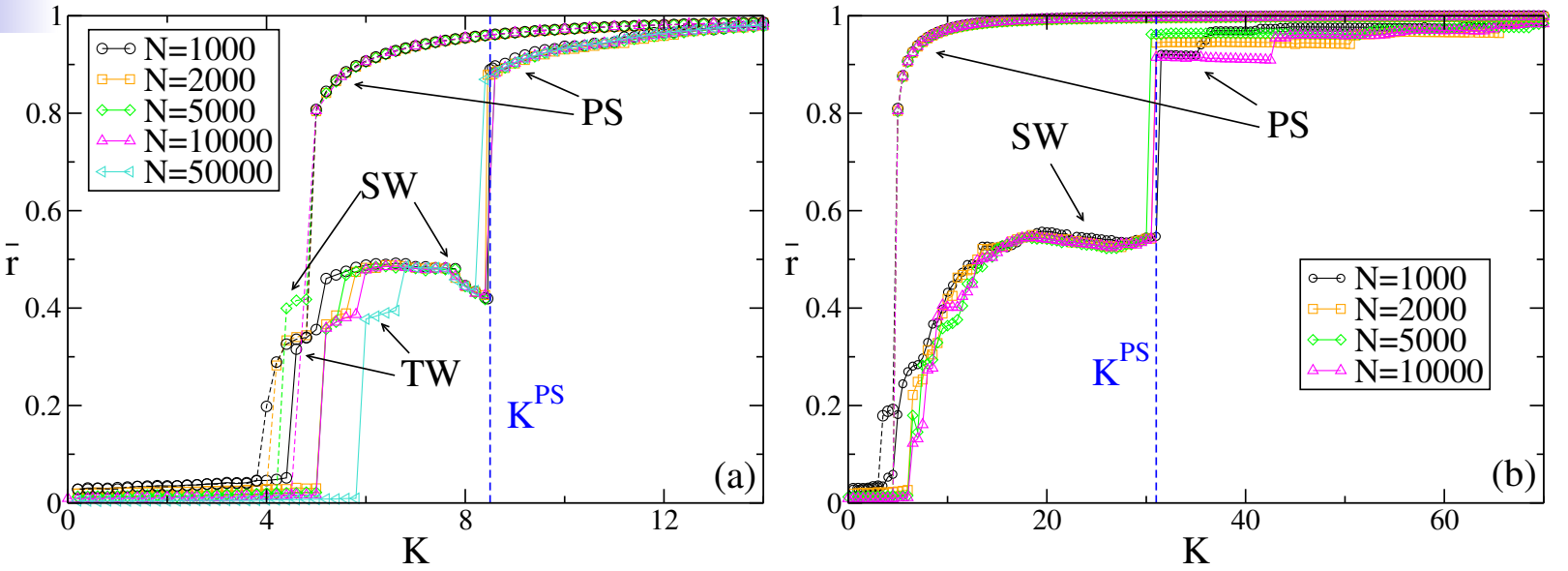

- Small inertia value
  - K^{TW} and K^{SW} increase with N
  - The transition value K^{PS} and K^{DS} seem independent from N
  - In the thermodynamic limit TW ans SW will be no more visited (the incoherent state will loose stability at K^{SW})
- Large inertia value
  - The transition to SW occurs via the emergence of clusters

Italian High Voltage Power Grid

Each node is described by the phase:

$$\phi_i(t) = \omega_{AC} t + \theta_i(t)$$

where $\omega_{AC} = 2\pi \ 50$ Hz is the standard AC frequency and θ_i is the phase deviation from ω_{AC}.

Consumers and generators can be distinguished by the sign of parameter P_i:

$$P_i > 0 \ (P_i < 0)$$

corresponds to generated (consumed) power.

$$\ddot{\theta}_i = \alpha \left[-\dot{\theta}_i + P_i + K \sum_{ij} C_{i,j} \sin(\theta_j - \theta_i) \right]$$

Average connectivity $< N_c >= 2.865$

[Filatrella et al., The European Physical Journal B (2008)]